Journal of Immunological Methods 405 (2014) 1–14

Contents lists available at ScienceDirect

Journal of Immunological Methods

journal homepage: www.elsevier.com/locate/jim

Research paper

Monoclonal antibody binding-site diversity assessment with a cell-based clustering assay

Sindy Liao-Chan, Joseph Zachwieja, Steven Gomez, Dana Duey, John Lippincott, Jan-Willem Theunissen *

Igenica Inc., 863 Mitten Road Suite 102, Burlingame, CA 94010, USA

ARTICLE INFO

Article history:
Received 5 October 2013
Received in revised form 12 December 2013
Accepted 19 December 2013
Available online 29 December 2013

Keywords:
Antibody sequencing
Biosensor
Clustering assay
Engineered cell lines
Epitope binning
Monoclonal antibody

ABSTRACT

The diversity of a panel of antibodies that target a specific antigen can be established in various assay formats. In conventional epitope binning assays purified antibodies are tested in a pairwise manner: two antibodies that compete with each other for binding to an antigen are grouped into the same cluster or bin, while they are assigned to two different clusters when they do not compete. Here we present a high through put assay that enables grouping of crude hybridoma supernatants without a need for antibody purification. In addition, the assay does not require recombinant protein, because it is conducted on cells that express the antigen of interest. Hence, one can use the antibody-clustering assay for cell surface proteins that are not amenable to purification. Heavy chain variable region (V_H) sequencing shows that V_H composition within clusters is conserved. Finally, the assay is in good agreement with a conventional epitope binning assay with purified antigen.

1. Introduction

Monoclonal antibodies (mAbs) are a rapidly growing category of targeted therapeutic agents against both soluble and cell surface proteins (Beck et al., 2010; Scott et al., 2012). MAbs are often generated with standard hybridoma technology, single B cell sequencing, or display technologies. Rodent species immunized with a human antigen (i.e. target) will develop B cells secreting antigen-specific antibodies. B cells can be fused with an immortal myeloma cell line to derive hybridoma cultures. Upon plating the hybridoma cultures in 96- or 384-well plates, crude culture supernatants are assayed for specificity to the human target. Because fusions can yield hundreds to thousands of target-specific hybridomas, screening methods are needed to identify a smaller subset of hybridomas for mAb purification and in-depth characterization. While these methods are often based on binding or functional effects of the mAbs, one widely used approach has been to identify diversity based on epitopes of the mAbs through cross-competition assays. Enriching for mAb binding-site diversity in early screening is beneficial, as mAbs with different epitopes can be functionally distinct (Dong et al., 2010; Koefoed et al., 2011; Niederfellner et al., 2011; Pedersen et al., 2010). In addition, identification of mAbs that can bind antigen simultaneously is valuable in designing reagents for other assays, such as immunogenicity or receptor occupancy assays (Byrd et al., 2012; Hellstrom et al., 1990).

Various epitope binning assays to screen for mAb binding site diversity exist. In classical sandwich ELISA experiments a mAb is immobilized, antigen is allowed to bind and after an incubation interval, a directly labeled mAb is added. If the immobilized mAb and directly labeled mAb do not compete for antigen binding, a signal is detected, and the mAbs are deemed to belong to

Abbreviations: AU, approximately unbiased; BLI, bio-layer interferometry; BSA, bovine serum albumin; CDR-H3, third complementarity-determining region of heavy chain; DPEP1, Dipeptidase 1; ELISA, enzyme-linked immunosorbent assay; FBS, fetal bovine serum; HRP, horseradish peroxidase; mAb, monoclonal antibody; mAb1, blocking antibody; mAb2, detection antibody; PBS, phosphate-buffered saline; SFM, serum-free media; V_H, heavy chain variable region

* Corresponding author. Tel.: +1 201 320 1495; fax: +1 650 697 4900.
E-mail addresses: sliaochan@igenica.com (S. Liao-Chan), jzachwieja@igenica.com (J. Zachwieja), sgomez@igenica.com (S. Gomez), dana.duey@gmail.com (D. Duey), lippy1@gmail.com (J. Lippincott), jtheunissen@igenica.com (J.-W. Theunissen).

0022-1759/$ – see front matter © 2013 Elsevier B.V. All rights reserved.
http://dx.doi.org/10.1016/j.jim.2013.12.007

different clusters. On the other hand, if the two mAbs compete for binding, no signal is detected and the mAbs are assigned to the same cluster. This classical ELISA or closely related formats cannot be deployed when using crude hybridoma supernatants, because the labeling reaction is usually performed with purified mAbs (Nakamura et al., 2012; Tsuji et al., 2012; Wagener et al., 1983). Clustering of crude mAb supernatants is possible with an ELISA in which an immune complex of two mAbs associated with an antigen is detected with an enzyme-linked reagent specific to a tag on the antigen (Nagata et al., 2004), or a multiplexed pairing assay (Jia et al., 2004; Miller et al., 2011). In one example of a multiplexed assay, mAbs are bound to Luminex beads via an anti-mouse IgG binding reagent (Miller et al., 2011). Each mAb is coupled to a different bead. Bead-labeled mAbs are incubated with antigen, followed by addition of a mAb that is probed with a phycoerythrin-labeled anti-mouse IgG binding reagent. Alternatively, mAb diversity in crude supernatants can be assayed with biosensors (Abdiche et al., 2012; Abdiche et al., 2009; Estep et al., 2013; Fagerstam et al., 1990; Shi et al., 2006). While the latter three assay formats are compatible with the use of crude hybridoma supernatants, these assays require purified antigen.

Here, we describe a screening assay for profiling mAb diversity of crude supernatants that does not require purified antigen. Instead, engineered cell lines expressing the human antigen of interest are used to assess mAb relatedness. Engineered cell lines have multiple advantages over purified human proteins. First, an antigen preparation that contains contaminants or non-native forms of the antigen could lead to selection of mAb candidates that bind biologically irrelevant epitopes (Abdiche et al., 2012). Second, some cell surface proteins, especially when containing multiple extracellular domains, are challenging to purify. Third, trans-membrane domains can be vital to the proper folding of the extracellular domain of membrane proteins, so only cell surface expression can capture the native conformation. In contrast to cell-based epitope binning assays with fluorescently conjugated purified mAbs (Ando et al., 2004; Fendly et al., 1990), the cell-based screening assay we developed does not require mAb purification and conjugation. In addition, the assay is relatively high-throughput in comparison to other protein- and cell-based clustering assays, as hundreds of crude supernatants can be screened.

2. Material and methods

2.1. Hybridoma and supernatant generation

129S6 mice (Taconic, Hudson, NY) were immunized with engineered murine sarcoma cells expressing human dipeptidase 1 (DPEP1). All experiments with mice were performed in accordance with Igenica's institutional guidelines and regulations. Five weeks post-immunization the cells were reinjected intraperitoneally and four days post-injection splenocytes were collected and fused with Sp2/mIL-6 myeloma cells (ATCC, Manassas, VA) using a standard polyethylene glycol (PEG) procedure. The fused cells were plated out in 384-well plates at a density that maximizes recovery of single hybridoma clones. One week after plating the hybridomas, colony counts indicated that >85% of wells with hybridomas only contained a single colony. DPEP1-specific hybridomas were selected by screening for binding to the cell line expressing human DPEP1 and not the parental line. Hybridomas were adapted to Hybridoma SFM (Life Technologies, Carlsbad, CA) supplemented with 5% Super Low IgG Fetal Bovine Serum (FBS; Thermo/Hyclone, Logan, UT), OPI (oxaloacetate, pyruvate, insulin) (Sigma, St. Louis, MO), Hypoxanthine-Thymidine (Mediatech/Cellgro, Manassas, VA).

To confirm that our 384-well plating strategy maximizes recovery of single hybridoma clones, we cloned all 22 IgG2a hybridomas used in Fig. 3A & B by limiting dilution. For each hybridoma, two 96-well plates were set up containing either 0.25 or 0.5 cells per well. On day 5 or 6 twelve wells containing single hybridomas were marked and on day 9 or 10 media from these wells were assayed by cell ELISA. Upon obtaining 2 to 3 separate 4 mL clonal supernatants for each IgG2a hybridoma, the cell-based clustering assay was conducted with a single clone for each IgG2a hybridoma. All cloned supernatants clustered in an identical manner compared to the supernatants used in Fig. 3A & B (Supplementary Fig. 1A & B, Fig. 3A & B).

2.2. Crude hybridoma supernatant characterization

Individual hybridoma supernatants incubated with the murine sarcoma cells expressing human DPEP1 were isotyped by using isotype-specific secondary antibodies (Goat anti-IgG1 Horseradish Peroxidase (HRP) — Jackson ImmunoResearch cat.# 115-035-206, Goat anti-IgG2a HRP — cat.# 115-035-206, Goat anti-IgG2b HRP — cat.# 115-035-207, Goat anti-IgG3 HRP — cat.# 115-035-209). The effective concentration of the hybridoma supernatants was measured by cell ELISA with a 4-point dilution series (1:4, 1:16, 1:64 & 1:256) of the supernatants and a murine Fc-specific secondary antibody (Jackson ImmunoResearch cat.# 115-035-071). Mouse IgG concentrations in the hybridoma supernatants were established with the Octet QK384 instrument (Fortebio, Menlo Park, CA) equipped with biosensors coated with goat anti-mouse IgG (Fortebio, part# 18-5024). A purified mAb spiked into culture media was used to establish a standard curve to calculate supernatant concentrations. Characterization of the hybridoma supernatants requires a relatively small cell number: isotyping, specificity assessment, and cell-based titration for 96 different hybridomas require a total of 6×10^6 cells when seeding 5×10^3 cells/well in 384-well plates. While isotyping and cell-based titration are conducted in singlet, specificity assessment is carried out in duplicate.

2.3. Hybridoma supernatant off-rate screening

Dissociation rates (off-rates) of the 43 anti-DPEP1 mAbs used in Figs. 3–6 & Supplementary Figs. 1–4 were established using the Octet QK384 with anti-mouse IgG Fc sensors (Fortebio, part# 18-5090) hydrated in Hybridoma SFM supplemented with 5% Super Low IgG FBS. Crude hybridoma supernatants were immobilized to the sensor surface for 2 min and a baseline step was recorded by moving the sensors to PBS pH 7.4 for 2 min. Association of the recombinant human DPEP1 protein (Sino Biological Inc., cat.# 13543-H08H; 100 nM in PBS pH 7.4) was measured for 4 min and dissociation was recorded by moving the sensors to PBS pH 7.4 for 10 min. Reference sensors were dipped in PBS during the association

step. The anti-mouse IgG Fc sensors were regenerated with three short cycles of alternating 15 second steps of 10 mM glycine-HCl pH 1.5 and PBS pH 7.4. The sample plate was pre-warmed at 27 °C for 10 min prior to initiation of the assay and agitated at 1000 rpm throughout the entire experiment. Data collected at 27 °C was aligned to the baseline step and reference sensor subtracted in Octet Data Analysis 7.0 software. Data was also inter-step corrected by alignment to the dissociation step and filtered using the Savitzky–Golay equation. Kinetic data was analyzed and fitted locally using a 1:1 Langmuir binding model. The $k_d(s^{-1})$, X^2 and R^2 were reported. X^2, a measurement of the goodness of curve fitting, is the sum of squared deviations, where deviation is the difference between the actual data point and the fitted curve. Values close to zero indicate a good curve fit. R^2, the coefficient of determination, is an estimate of the goodness of the curve fit and is not directly related to the estimate of a specific parameter. Values close to 1.0 indicate a good curve fit.

2.4. Cell-based clustering assay

Murine sarcoma cells expressing DPEP1, seeded in 384-well plates at 5×10^3 cells/well, were incubated at room temperature with media or a mAb (mAb1) of a certain isotype (e.g. IgG1/2b) at a dilution previously determined to be 10× that required for saturation (Supplementary Table 1). We refer to mAb1 as a blocking mAb, because it potentially hinders binding of a second mAb. After 1 h, the cells were washed three times with PBS supplemented with 0.1% BSA, fixed with 1% paraformaldehyde in PBS for 10 min, and washed three times with PBS 0.1% BSA. Next, the cells were incubated at room temperature for 1 h with either media or a detection mAb (mAb2) of another isotype (e.g. IgG2a). For the 43 DPEP1 blocking mAb1's and detection mAb2's used in the reproducibility experiments a median amount of 4 pmol [20 μl at 30 μg/ml] and 0.4 pmol [20 μl at 3 μg/ml], respectively, was used per well (Supplementary Table 2). After three washes with PBS 0.1% BSA, the wells were incubated for 30 min at room temperature with a secondary antibody conjugated to HRP specific for the detection mAb (e.g. IgG2a) and detected with SuperSignal ELISA Pico Chemiluminescent Substrate (Thermo Scientific part# 37069). The fixation, and washes prior to and after the fixation, can be omitted, without affecting the outcome of the clustering assay for the 43 DPEP1 mAbs used in the reproducibility experiments (Supplementary Fig. 1C & D). The mAb2 luminescence data for each mAb2–mAb1 pair was divided by the mAb2 luminescence data for wells incubated with media and mAb2 only, and this fraction was multiplied by one hundred to obtain a percentage of the control value. These normalized luminescence data are tabulated in a two-dimensional matrix. In addition, the assay included control-wells that were only incubated with the blocking mAbs and presence of these blocking mAbs was detected with the appropriate isotype-specific HRP-conjugated secondary antibodies. When detecting blocking IgG1/2b mAbs, a 1:1 mixture of the anti-IgG1 HRP and the anti-IgG2b HRP conjugates was used. The clustering assay requires a relatively small cell number: profiling 22 blocking mAbs against 84 detection mAbs, requires a total of 12×10^6 cells when seeding 5×10^3 cells/well in 384-well plates.

2.5. Biosensor-based clustering assay

Amine-reactive second generation sensors (AR2G) on an Octet QK384 instrument (Fortebio, Menlo Park, CA) were equilibrated in water for 1 min and then activated with a freshly prepared mixture of 20 mM EDC (1-Ethyl-3-[3-dimethylaminopropyl] carbodimide hydrochloride) and 10 mM sulfo-NHS (N-hydroxysulfosuccinimide) for 5 min. At a 100 nM concentration in 10 mM sodium acetate pH 6 buffer, recombinant human DPEP1 antigen (Sino Biological Inc., cat.# 13543-H08H) was covalently immobilized through NHS/EDC coupling chemistry on the sensors for 4 min with a mean immobilization level of 1.84 (± 0.29) nm, and excess reactive esters were quenched with 1 M ethanolamine pH 8.5 for 5 min. Antigen-coated sensors were then dipped in PBS for 1 min to record a baseline step. Next, the antigen-coated sensors were dipped in one blocking mAb (mAb1) and binding was measured until saturation for 10 min. The blocking mAb1-antigen coated sensors were washed for 15 s in PBS, and then moved to wells containing an array of detection mAbs (mAb2's) and binding was measured for 5 min. Antigen-coated tips were regenerated with 3 short cycles of 20 second alternating steps of Gentle Ab/Ag Elution Buffer pH 6.6 (Thermo Scientific cat.# 21013) and PBS. The assay was repeated with the same mAb1 with a new array of mAb2's. Antigen-coated sensors were used and regenerated three times before a new set of sensors was used. On control sensors, media replaced mAb1 and/or mAb2. Octet binding data was analyzed and processed using Octet Data Analysis 7.0 software. For all binding steps, data was aligned to zero (baseline) on both the *x*- and *y*-axes. No referencing was applied. To obtain a percentage of the control response, the mAb2 binding response for each mAb2-mAb1 pair was divided by the mAb2 binding response for the biosensor incubated with media and mAb2 only. The normalized binding responses are tabulated in a two-dimensional matrix.

2.6. Analysis of clustering data

To compare antibodies in the two-dimensional matrices, the relative luminescence data from the cell-based clustering assay or the relative binding data from the biosensor-based clustering assay were plotted such that the detection mAbs (mAb2's) were in rows and the blocking mAbs (mAb1's) were in columns. The initial position of the antibodies in these two-dimensional matrices was based on the order of addition of the antibody supernatants to the 384-well cell ELISA plate or the biosensor. Pearson correlation coefficients were calculated using the PEARSON function in Microsoft Excel as described (Miller et al., 2011). Briefly, after calculating the Pearson correlation coefficients of the leftmost column and every other column, the column with the highest correlation was placed to the right of the first column. These calculations were repeated for all the other columns in the matrix, and the same calculations were applied on the rows in the matrix. The antibody in the leftmost column and the antibody in the top row affect the order of the antibodies in the Pearson-sorted two-dimensional matrix. The unsorted data in the two-dimensional matrices was also imported into R (The R Project for Statistical Computing (www.r-project.org); with

addition of the R package pvclust) to generate a clustergram (Suzuki and Shimodaira, 2006). Note that the data is transposed prior to being imported into R, i.e. the mAb2's are in separate columns and the mAb1's are in separate rows. An example R script that sources data stored in a comma-separated values file named "data.csv" is provided: line1: library (pvclust); line2: data < − read.table("/Desktop/data.csv, header = TRUE, row.names = 1, sep=","); line3: result < − pvclust(data, nboot = 10000); line4: plot(result); line5: pvrect (result, alpha = 0.95).

2.7. V_H sequencing

Heavy chain variable region sequencing was conducted as described (Jones and Bendig, 1991). One microgram of RNA was reverse transcribed with oligo-dT primers and Superscript III (Life Technologies, Carlsbad, CA). PCR amplification of the heavy chain variable regions was conducted with the 5′ and 3′ primer sets as described (Jones and Bendig, 1991). Sequence analysis was conducted with Lasergene 9 (DNAStar, Madison, WI). The phylogram was generated using the ClustalW Method in MegAlign (DNAStar). For each mAb, VBASE2 was used to derive the V_H family, the V_H and J_H genes, and the CDR-H3 sequence (Retter et al., 2005). Light chain sequencing was not conducted in this study.

3. Results

3.1. Overview of the cell-based clustering assay

The cell-based clustering assay is based on sequential binding of two hybridoma supernatants to an engineered murine sarcoma cell line that expresses a human target of interest and takes advantage of the use of isotype-specific detection. Other engineered cell lines or endogenous expressing cell lines amenable to cell-based ELISA can also be used. The isotype of the first blocking mAb (mAb1; e.g. IgG1 or IgG2b [abbreviated as IgG1/2b]) is different from the isotype of the second detection mAb (mAb2; e.g. IgG2a). Binding of mAb2 to cells is detected by adding an isotype-specific HRP-conjugated secondary polyclonal antibody (Fig. 1A). HRP luminescence indicates that mAb1 and mAb2 can simultaneously bind to the cell surface-expressed human target. A reduction of HRP luminescence compared to the control (no mAb1), on the other hand, shows that the binding of mAb1 interferes with the concurrent binding of mAb2.

Crude hybridoma supernatants with different IgG isotypes are used for the cell-based clustering assay. Before conducting the assay, hybridoma supernatants are titrated and surveyed for specificity and isotype. Specificity is established by screening the supernatants on the engineered cell line that expresses the human target of interest and the parental cell line. Crude supernatants are specific when they only stain the engineered cell line with the human target. Supernatant isotype is established with the isotype-specific HRP-conjugated secondary antibodies used in the cell-based clustering assay. A four-point titration on the engineered cell line is conducted to establish at what dilution the supernatant saturates staining. Specific, single-isotype hybridoma supernatants are grouped according to isotype. The blocking mAbs (mAb1; e.g. IgG1/2b) are used at a dilution that is 10-fold greater than the saturating dilution, whereas the detection mAbs (mAb2; e.g. IgG2a) are used at the saturating dilution (Supplementary Table 1).

To establish mAb relatedness, the luminescence data for all the mAb2–mAb1 pairs is divided by the luminescence data from the wells incubated with media and mAb2 only and the fractions are multiplied by one hundred. This normalized data is tabulated in a two-dimensional matrix and used to derive a mAb2–mAb1 cell ELISA clustergram (e.g. [a mAb2 [IgG2a]–mAb1[IgG1/2b] clustergram]; Fig. 1). In the two-dimensional matrix the mAb1's and the mAb2's are sorted based on the Pearson product-moment correlation coefficients of the normalized data (Fig. 1B). On the other hand, the mAb2–mAb1 clustergram (Fig. 1C) shows the relatedness of the mAb2's by means of hierarchical clustering and *p*-value reporting. The *y*-axis of the clustergram – Height – is a measure of dissimilarity between mAb2's. MAb2's belong to the same cluster when their binding profiles in the presence of different mAb1's are similar. AU (Approximately Unbiased) *p*-values are computed by multi-scale bootstrap resampling (Suzuki and Shimodaira, 2006). For clusters with an AU *p*-value cut-off above 95 the hypothesis that the cluster does not exist is rejected with a 0.05 significance level. Clusters are defined top-down below a manually set Height cut-off on the *y*-axis, so that clusters do not contain highly dissimilar mAbs. For example, with a Height cut-off of 1, the first eight mAb2's (mAb2_1, 2, 3, 4, 5, 6, 7 & 8) would all fall into one cluster that is dissimilar from the cluster that contains mAb2_9 & mAb2_10 (Fig. 1C). However, the blocking profiles for these first eight mAb2's are different when inspecting the two-dimensional matrix, indicating that the cluster contains dissimilar mAb2's (Fig. 1B). When clusters are defined top-down below a Height cut-off of 0.1, four clusters emerge (Fig. 1C). Within each of these four clusters, the blocking profiles are similar. For example, cluster 1 mAb2's are blocked by mAb1_3, mAb1_4, mAb1_5, mAb1_6 & mAb1_7, while cluster 4 mAb2's are blocked by mAb1_8, mAb1_9 & mAb1_10. In addition, the Pearson correlation coefficient between mAb2 pairs is only greater than 0.9 within each cluster, not between clusters. While a Height cut-off that is too high results in clusters containing dissimilar mAbs, a Height cut-off that is too low results in assignment of similar mAbs to different clusters. For example, when the Height cut-off is set at 0.01, mAb2_3 is assigned to its own cluster (Fig. 1C). However, the mAb2_3 blocking profile is very similar to the mAb2_1 and mAb2_2 blocking profiles, i.e. the blocking profiles vary only by 10% in cluster 1 (Fig. 1B). Small differences in normalized luminescence data can be ascribed to noise in the assay. In summary, manual inspection of the normalized luminescence data and the Pearson correlation coefficients should be used to establish appropriate Height and AU *p*-value cut-offs. During later stages of mAb diversity assessment the Height and AU *p*-value cut-offs can be adjusted by assessing assay reproducibility and conducting V_H sequencing (Sections 3.2 & 3.3, respectively).

An important attribute of the cell-based clustering assay is that detection mAb2's of a particular isotype (e.g. IgG2a) can only be profiled against blocking mAb1's of a different isotype (e.g. IgG1/2b). Because the high-throughput cell-based clustering assay enables profiling of a large collection of blocking mAb1's against a large collection of detection mAb2's, the success of the assay relies on the presence of mAbs with similar

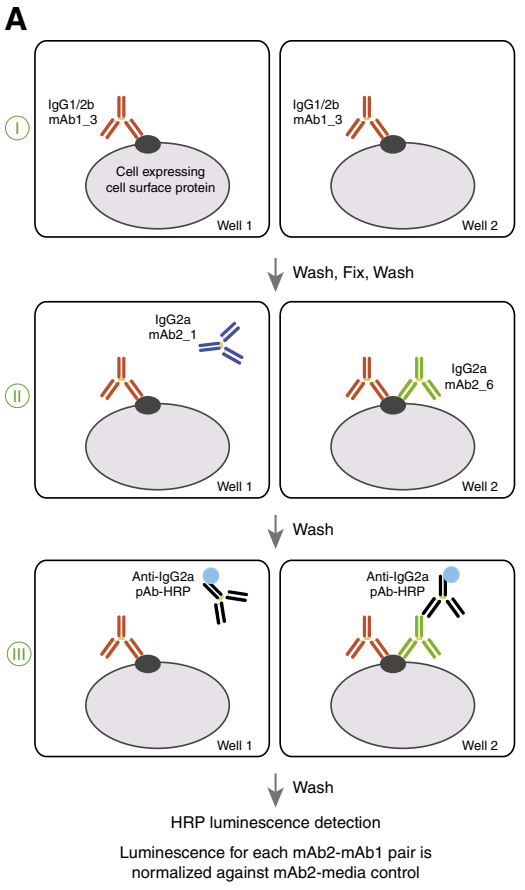

B

#	mAb2 \ mAb1	mAb1_1	mAb1_2	mAb1_3	mAb1_4	mAb1_5	mAb1_6	mAb1_7	mAb1_8	mAb1_9	mAb1_10	Pearson	mAb2-mAb1 cell-ELISA cluster
1	mAb2_1	50	50	5	5	5	20	20	100	100	100		1
2	mAb2_2	45	45	5	5	5	15	15	100	100	100	1.00	1
3	mAb2_3	50	50	5	5	5	15	15	100	100	100	1.00	1
4	mAb2_4	100	100	1	1	1	90	90	100	100	100	0.70	2
5	mAb2_5	100	100	1	1	1	100	100	100	90	90	0.99	2
6	mAb2_6	100	100	100	100	100	20	20	100	100	100	-0.36	3
7	mAb2_7	100	100	100	100	100	15	15	95	95	95	1.00	3
8	mAb2_8	100	100	95	95	95	13	13	100	100	100	0.99	3
9	mAb2_9	95	95	95	95	95	95	95	1	1	1	-0.36	4
10	mAb2_10	90	90	90	90	90	90	90	2	2	2	1.00	4
	Pearson		1.00	0.59	1.00	1.00	-0.07	1.00	-0.59	1.00	1.00		

C

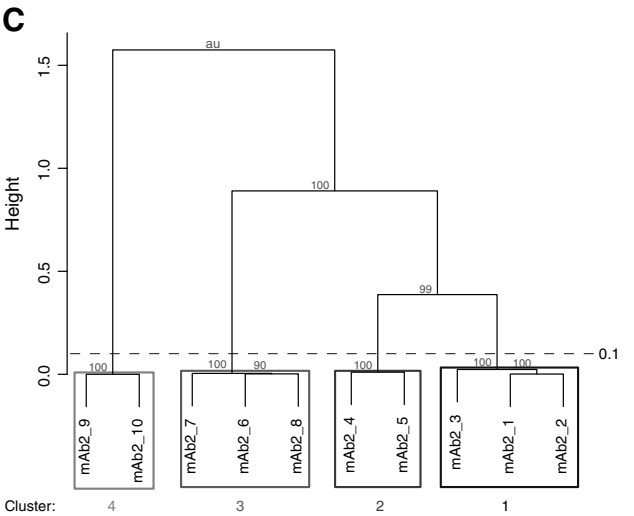

Fig. 1. Schema of cell-based clustering assay using artificial dataset. (A) Overview of the cell-based clustering assay. Murine cells expressing a human target of interest in two different wells are incubated with the target-specific IgG1/2b blocking mAb1_3 (orange mAb in step I). After a wash, a fixation step, and another wash, the cells are incubated with two different target-specific IgG2a mAb2's: mAb2_1 in well 1 & mAb2_6 in well 2 (blue and green mAb, respectively, in step II). Only mAb2_6 can bind the target in the presence of mAb1_3. After a wash, bound IgG2a mAb2 is detected with an IgG2a-specific HRP-conjugated secondary antibody (black mAb in step III). The secondary antibody only detects mAb2_6 in well 2. Hence, mAb2_1 and mAb2_6 belong to different clusters. (B) A two-dimensional matrix with artificial normalized luminescence data for 10 hypothetical IgG2a detection mAb2's and 10 hypothetical IgG1/2b blocking mAb1's. Pearson correlation coefficients for the blocking mAb1 and its left-side neighbor and for the detection mAb2 and its upper neighbor are shown at the bottom and at the right side of the matrix, respectively. A gray gradient is applied to normalized data between 0 (gray) and 100 (white) to highlight mAb1 blocking. (C) Clustergram for 10 IgG2a detection mAbs. The axis on the left side of the clustergram named "Height" is a measure of dissimilarity between the 10 mAb2's and their clusters. AU *p*-value cut-offs are shown in gray. Four mAb2–mAb1 clusters emerged at an AU *p*-value cut-off at 95 and a Height cut-off at 0.1.

epitopes, but different isotypes in the hybridoma collection. Indeed, this assumption is consistent with the mechanisms of B-cell development during a humoral immune response, where the same or very similar paratopes are expected to be found in different IgG isotype classes (Keim et al., 2013). It is also possible to carry out the assay in a reciprocal format, i.e. the blocking mAb1's can be used as detection mAb2's and vice versa. If the first assay is conducted with IgG1/2b blocking mAb1's and IgG2a detection mAb2's, the second assay is conducted with IgG2a blocking mAb1's and IgG1/2b detection mAb2's.

3.2. Cell-based clustering assay for the cell surface protein DPEP1

To demonstrate the high-throughput nature of the assay we profiled 115 crude hybridoma supernatants: 31 IgG1/2b blocking mAb1's against 84 IgG2a detection mAb2's. All hybridomas were derived from immunizations in 129S6 mice using a murine sarcoma cell line expressing human dipeptidase 1 (DPEP1) (Keynan et al., 1997; Matsushita et al., 2012; Toiyama et al., 2011). DPEP1 is a predicted glycosylphosphatidylinositol-anchored 411 amino acid surface protein. The hybridomas were obtained from 3 different fusions that used splenocytes from different mice — R48C1-67, R48C2-34 and R48C2-5. Prior to clustering, supernatant specificity was confirmed, and supernatant isotype was used to group the IgG1/2b supernatants as blocking mAb1's and the IgG2a supernatants as detection mAb2's. The dilutions to use in the clustering assay were determined by titrating the supernatants on the engineered murine cell line expressing DPEP1 (Supplementary Table 1). The supernatants were then used in the clustering assay by incubating the DPEP1-expressing cell line with the blocking mAb1's or media, followed by incubation with the detection mAb2's. Once the luminescence data was obtained with the IgG2a-specific HRP-conjugated secondary antibody,

the mAb2–mAb1 data was normalized against the wells incubated with media and mAb2, and this normalized data set was subsequently used to construct a two-dimensional matrix (Fig. 2A) and clustergram (Fig. 2B). Upon manual inspection of the blocking profiles and the Pearson correlation coefficients, we defined clusters top-down below a Height cut-off at 0.3 with an AU *p*-value cut-off at 90. At these cut-offs, four mAb2[IgG2a]–mAb1[IgG1/2b] cell ELISA clusters emerged and three mAbs – R48C2-34-32, R48C1-67-18 & R48C1-67-19 – were not assigned to a cluster. Furthermore, with eight exceptions (rows 54, 56, 64, 67, 79 up to 82), the Pearson correlation coefficients between mAbs within each cluster were greater than 0.9 (Fig. 2A).

Instead of solely setting cut-offs based on manual inspection of the blocking profiles and the Pearson correlation coefficients, we established whether assay reproducibility could be used to set the Height and AU *p*-value cut-offs. To do so, we chose a defined, smaller subset of crude supernatants from the two-dimensional matrix – 21 blocking mAb1's and 22 detection mAb2's (bold font and marked with an asterisk in Fig. 2). This smaller set was also used to assess relatedness of IgG1/2b's, to establish mAb diversity by V_H sequencing, and to benchmark the cell-based assay against a biosensor-based assay (Sections 3.2, 3.3 & 3.4, respectively). The selected detection mAb2's fell into mAb2[IgG2a]–mAb1[IgG1/2b] cell ELISA clusters 1 & 2 or were not assigned to a cluster (as is the case for R48C1-67-18 and R48C1-67-19), whereas the selected blocking mAb1's represented a comprehensive set that recapitulated different profiles of blocking for the various detection mAb2's (Fig. 2A). Newly made crude supernatants for these 43 mAbs were titrated, and isotype and specificity was reconfirmed (Supplementary Table 2). Median mAb concentration in the supernatants was 128 μg/ml (with a minimum and maximum of 34 and 269 μg/ml, respectively) (Supplementary Table 2). The cell-based clustering assay was carried out twice on different days in the same format — 21 IgG1/2b mAb1's profiled against 22 IgG2a mAb2's. The median concentrations for mAb1 and mAb2 were 30 and 3 μg/ml, respectively (Supplementary Table 2). When clusters were defined top-down below a Height cut-off at 0.1 with an AU *p*-value cut-off at 95, three identical mAb2[IgG2a]–mAb1[IgG1/2b] clusters were present in both replicate clustering assays (Fig. 3A & B, Supplementary Fig. 2A & B). All the antibodies that fell into clusters 1 & 2 in Fig. 3B exhibited the same clustering pattern in Fig. 2B. Two mAbs – R48C1-67-18 and R48C1-67-19 – were not assigned to a cluster in Fig. 3B, because they were dissimilar on the *y*-axis (i.e. above the 0.1 Height cut-off), matching the lack of assignment in Fig. 2B. Finally, two other mAbs – R48C2-34-04 and R48C2-34-43 – were assigned to cluster 5 (Fig. 3B & Supplementary Fig. 2B). R48C2-34-04 and R48C2-34-43 fell into cluster 1 in the 84 mAb2–31 mAb1 clustergram (Fig. 2B), suggesting that the cut-offs in this larger clustergram should be adjusted. In summary, assay reproducibility can be used in addition to inspection of the two-dimensional matrix to set the Height and AU *p*-value cut-offs.

We also conducted the cell-based clustering assay twice in its reciprocal format to understand the relatedness of the IgG1/2b mAbs. Despite small differences between the replicate experiments, assay reproducibility was used to set the Height and AU *p*-value cut-offs, with 18 out of 21 IgG1/2b exhibiting identical assignments. Fifteen out of 21 IgG1/2 mAb2's fell into mAb2 [IgG1/2b]–mAb1[IgG2a] clusters *a*, *b* & *c* (Fig. 3D, Supplementary Fig. 2D), whereas 3 out of 21 IgG1/2b mAb2's – R48C1-67-21, R48C2-34-80 and R48C2-5-109 – did not fall into clusters, as these 3 mAbs appeared to be unique when inspecting the two-dimensional matrices and clustergrams (Fig. 3C & D, Supplementary Fig. 2C & D). When used as blocking mAb2's in Fig. 2A, the 3 unassigned IgG1/2b mAbs stood out as the mAbs with the lowest Pearson correlation coefficients (<0.36) relative to all other IgG1/2b blocking mAb1's. In the second replicate experiment conducted on a different day, one mAb2 – R48C1-67-90 – was not assigned to cluster *b* (Supplementary Fig. 2C & D) and two other mAbs – R48C1-67-09 & R48C1-67-41 – were defined as mAbs that fell into cluster *d* (Supplementary Fig. 2D). R48C1-67-90 was assigned to cluster *b* in Section 3.3, because all cluster *b* mAb2's – including R48C1-67-90 – were blocked by R48C2-34-04 and R48C2-34-43 by at least 90% (Fig. 3C, Supplementary Fig. 2C). Because the blocking profiles for R48C1-67-09 & R48C1-67-41 were similar to the profiles for the other mAb2's in cluster *a* (Fig. 3C, Supplementary Fig. 2C), both mAbs were considered part of cluster *a* in Section 3.3.

While the cell-based assay allows mAb binding-site diversity clustering within isotype classes, relatedness between isotype classes can be determined by inspecting the cluster assignments listed in the second-to-last column and the last row of the two-dimensional matrices (Fig. 3A & C). We considered mAb2[IgG2a]–mAb1[IgG1/2b] clusters (clusters 1, 2, & 5; assignment based on clustergram in Fig. 3B) akin to mAb2[IgG1/2b]–mAb1[IgG2a] clusters (*a*, *b* & *c*; assignment based on clustergram in Fig. 3D) when at least half of the blocking mAb1's from a particular cluster blocked the detection mAb2's of a particular cluster by at least 50% (relationships listed in last column of two-dimensional matrix in Fig. 3A & C). For example, cluster 1 was related to cluster *a*, because 8 out of 11 blocking mAb1's from cluster *a* blocked the antibodies in cluster 1 by at least 50% (last column of two-dimensional matrix in Fig. 3A). Relatedness between isotype classes is discussed further in Section 4.2.

3.3. Relationship between cell-based clusters and heavy chain variable region sequences

While the epitope is the portion of the antigen that is recognized by a mAb, the paratope is the antigen-binding site of the mAb. The highest sequence diversity of antibodies occurs within the third complementarity-determining region of the heavy chain (CDR-H3), with CDR-H3 loops located in the center of the antigen-binding site (Murphy et al., 2008). The CDR-H3 of a mAb specifies the V_H clonotype, a group of V_H sequences that

Fig. 2. Cell-based clustering assay for 84 IgG2a detection mAb2's using 31 IgG1/2b blocking mAb1's.(A) A two-dimensional matrix with the normalized luminescence data for 84 IgG2a detection mAb2's and 31 IgG1/2b blocking mAb1's against DPEP1. Pearson correlation coefficients for the blocking mAb1 and its left-side neighbor and for the detection mAb2 and its upper neighbor are shown at the bottom and at the right side of the matrix, respectively. (B) Clustergram for 84 IgG2a detection mAbs with 4 clusters defined at an AU *p*-value cut-off at 90 and a Height cut-off at 0.3. Data display and gray scaling as in Fig. 1. The blocking and detection mAbs used for validation of the assay are highlighted in bold and marked with an asterisk (*).

A

	mAb2 \ mAb1	1 R48C1-67-5	2 R48C1-67-10	3 R48C1-67-56	4 R48C1-67-46*	5 R48C1-67-20*	6 R48C1-67-73	7 R48C1-67-77	8 R48C1-67-88*	9 R48C1-67-34*	10 R48C1-67-8*	11 R48C1-67-53*	12 R48C2-34-69*	13 R48C2-34-10	14 R48C2-34-143	15 R48C2-5-27	16 R48C1-67-21*	17 R48C1-67-41*	18 R48C1-67-9*	19 R48C2-5-109*	20 R48C2-34-126*	21 R48C2-34-107	22 R48C2-34-30*	23 R48C1-67-89*	24 R48C1-67-90*	25 R48C1-67-33*	26 R48C1-67-49*	27 R48C2-34-75*	28 R48C2-34-42*	29 R48C2-34-6*	30 R48C2-34-36	31 R48C2-34-80*	Pearson	mAb2-mAb1 cell-ELISA cluster
1	**R48C1-67-2***	4	5	12	23	8	6	7	19	23	53	11	15	10	13	10	5	10	7	103	68	42	59	77	75	88	82	80	78	71	77	116		1
2	**R48C1-67-4***	6	8	17	28	12	8	9	21	27	56	15	19	14	16	9	8	11	8	96	75	50	78	88	89	99	96	94	86	77	85	117	0.99	1
3	R48C1-67-15	8	7	16	26	11	7	9	19	27	69	14	16	14	12	10	7	12	7	93	68	42	71	101	100	95	94	89	87	97	87	122	0.99	1
4	R48C1-67-35	8	7	16	30	12	8	8	22	34	68	15	16	15	18	13	7	11	8	97	76	56	70	115	119	110	105	91	101	109	97	145	1.00	1
5	R48C1-67-13	5	6	12	22	9	7	7	16	28	58	12	13	12	12	8	6	9	7	101	66	39	57	93	98	112	103	97	86	101	92	135	0.99	1
6	R48C1-67-7	4	4	10	17	7	6	6	12	19	39	9	11	8	8	6	6	6	4	89	69	35	61	95	88	91	91	93	81	86	95	126	0.99	1
7	R48C1-67-27	1	1	3	9	4	2	3	8	12	34	3	6	4	6	3	4	2	1	103	71	29	57	101	101	94	88	91	88	96	98	133	1.00	1
8	**R48C1-67-37***	6	5	10	19	8	6	6	13	18	52	9	12	11	11	11	7	6	4	101	76	41	83	127	123	102	100	100	99	115	109	134	0.99	1
9	R48C1-67-30	6	5	11	21	9	7	7	16	22	53	10	13	15	14	13	8	7	5	93	82	48	102	133	133	93	98	97	106	125	115	133	0.99	1
10	**R48C2-5-3***	16	13	21	40	18	13	15	31	40	90	22	26	22	27	16	16	15	25	96	75	57	92	113	115	105	101	95	110	121	122	105	0.97	1
11	R48C2-5-7	13	15	21	40	18	14	14	30	39	76	19	19	15	21	13	15	14	15	105	68	48	68	105	112	102	99	97	106	115	109	98	0.99	1
12	R48C2-5-5	14	15	20	39	18	12	17	28	40	79	20	25	21	23	14	14	15	16	108	88	58	94	129	110	95	91	93	107	111	129	93	0.98	1
13	**R48C1-67-43***	5	4	11	24	7	7	8	19	25	44	11	16	10	14	9	7	9	5	102	79	36	65	94	92	101	105	106	113	87	111	98	0.96	1
14	**R48C1-67-40***	5	5	15	29	8	8	8	23	30	49	14	18	13	18	10	6	12	6	106	80	42	65	85	90	96	109	101	110	83	110	93	1.00	1
15	**R48C1-67-44***	5	5	14	29	8	7	7	21	28	51	15	15	9	14	9	5	10	6	101	77	35	56	75	78	96	99	91	99	77	111	86	1.00	1
16	R48C1-67-47	4	3	10	23	6	5	6	14	21	39	10	11	8	10	7	5	8	4	96	69	29	47	82	82	101	104	96	92	80	108	97	0.99	1
17	R48C1-67-50	2	2	9	13	4	4	3	9	16	30	6	9	5	8	3	4	4	2	96	67	22	50	85	81	106	102	99	101	74	116	91	1.00	1
18	R48C1-67-23	3	3	9	19	6	5	7	17	20	38	8	12	7	9	4	5	7	4	94	57	24	41	66	70	98	93	95	89	66	87	81	0.99	1
19	R48C1-67-22	4	3	12	23	8	6	6	18	24	48	10	12	8	10	5	6	9	5	102	66	27	40	75	71	116	106	93	87	71	88	96	0.99	1
20	R48C1-67-16	2	2	5	11	3	2	3	6	10	22	5	6	3	4	3	2	4	1	90	41	14	23	71	72	104	111	94	88	74	97	95	0.98	1
21	R48C1-67-14	5	6	12	21	8	9	8	14	21	42	11	11	9	9	7	10	8	5	99	83	35	73	85	101	94	106	90	81	86	93	136	0.95	1
22	**R48C1-67-3***	9	9	13	23	13	6	7	17	26	82	12	16	12	12	13	7	11	13	99	74	47	72	97	90	110	98	91	86	92	94	126	0.98	1
23	R48C2-34-40	14	17	24	39	23	18	17	34	46	75	90	28	26	28	15	22	21	15	100	75	61	83	105	109	101	93	92	85	105	95	115	0.93	1
24	**R48C2-34-45***	15	16	21	35	23	18	17	31	43	70	100	27	24	22	16	21	20	16	100	76	60	78	114	107	107	98	86	82	103	100	118	0.99	1
25	R48C2-34-16	17	14	21	35	21	15	15	29	40	80	100	29	23	25	17	19	18	14	98	79	59	81	107	110	102	90	89	85	96	91	125	0.99	1
26	R48C2-5-55	18	15	18	36	20	16	15	29	40	84	30	30	26	22	19	19	18	16	100	78	61	82	122	122	102	101	91	93	110	97	128	1.00	1
27	R48C2-5-51	18	14	19	33	21	15	15	30	39	79	104	29	26	22	21	17	18	15	96	78	58	81	122	116	104	92	92	90	97	97	117	1.00	1
28	R48C2-5-20	20	16	24	34	22	17	18	32	38	81	97	32	29	26	22	19	19	16	92	73	57	82	112	109	88	100	82	88	101	95	109	0.99	1
29	R48C2-5-17	19	16	21	35	19	15	16	32	40	88	98	33	31	26	19	20	17	15	93	77	59	85	119	119	94	95	94	95	112	93	126	1.00	1
30	R48C2-5-58	20	17	23	40	23	17	18	33	42	81	104	33	32	33	23	21	20	16	106	88	67	85	125	124	102	91	94	99	119	98	138	1.00	1
31	R48C2-5-52	20	18	22	41	24	16	17	32	40	87	118	27	27	27	21	19	19	18	105	86	68	85	124	120	107	91	97	91	118	101	137	1.00	1
32	R48C2-5-57	19	19	22	41	25	16	18	32	40	87	114	33	28	26	21	19	18	16	110	87	70	84	114	116	102	100	90	94	117	101	132	1.00	1
33	R48C2-5-25	22	14	21	39	23	15	16	32	43	99	113	29	25	25	17	18	17	12	106	83	61	80	124	116	103	106	91	96	114	102	134	1.00	1
34	R48C2-34-49	15	15	22	43	22	16	17	36	46	87	106	31	26	26	15	15	20	15	102	74	57	84	113	112	93	93	89	92	109	102	120	0.99	1
35	**R48C2-5-12***	20	16	20	36	22	14	15	30	41	89	112	36	34	28	19	17	20	17	102	74	70	92	128	127	100	90	98	100	120	111	113	0.99	1
36	R48C2-34-39	7	8	8	16	13	9	9	13	20	42	16	10	8	6	6	14	6	5	87	50	23	57	111	124	116	99	87	89	95	106	100	0.95	1
37	R48C2-34-27	16	9	20	36	14	14	14	32	43	61	95	26	15	18	12	14	13	7	90	74	37	51	92	84	103	90	88	89	74	95	89	0.96	1
38	R48C2-5-35	17	13	25	41	17	18	18	36	46	67	101	35	26	32	18	16	18	10	100	81	50	63	98	83	96	102	96	100	79	105	96	0.99	1
39	R48C2-5-30	14	14	25	42	16	16	17	35	46	70	113	32	25	30	15	15	19	9	105	82	52	66	92	93	104	106	98	106	86	109	93	1.00	1
40	R48C2-5-45	13	8	22	39	16	13	15	31	40	61	103	35	23	33	13	12	17	9	98	90	49	62	84	85	95	93	92	96	82	103	88	1.00	1
41	R48C2-34-88	14	12	22	38	18	17	17	32	43	61	91	34	21	30	12	14	21	11	101	80	38	64	81	78	90	86	90	92	75	104	78	0.99	1
42	R48C2-34-25	17	8	19	40	13	12	14	28	37	57	95	26	19	25	12	11	15	8	96	75	42	58	85	68	89	89	84	83	71	96	88	0.99	1
43	R48C2-34-65	28	9	21	39	16	15	15	33	41	55	95	27	18	27	12	12	19	9	102	81	47	63	81	75	95	96	83	84	73	99	104	0.99	1
44	R48C2-5-33	13	12	24	39	15	16	16	33	41	69	100	33	21	30	14	15	18	11	101	86	46	57	86	83	95	96	81	83	71	94	92	0.99	1
45	R48C2-34-23	14	12	24	39	18	17	17	35	48	75	107	31	21	27	15	15	21	11	98	87	43	61	80	87	104	95	88	97	77	100	90	0.99	1
46	R48C2-34-55	11	12	26	45	18	16	19	39	54	67	101	35	23	35	15	13	23	12	101	84	52	62	73	78	91	80	88	91	79	102	83	0.99	1
47	R48C2-34-135	8	8	17	30	14	13	14	25	38	48	106	19	14	20	9	13	16	6	96	79	40	56	83	77	92	87	94	92	77	102	79	0.98	1
48	R48C2-34-56	15	14	28	48	21	21	22	42	51	66	106	35	25	32	16	17	25	14	91	81	37	59	79	85	103	102	87	95	73	108	62	0.98	1
49	**R48C2-34-8***	11	11	25	49	14	14	15	32	47	57	68	26	14	26	10	10	17	11	104	89	45	66	83	85	103	111	97	112	85	125	60	0.96	1
50	**R48C2-34-9***	10	9	26	43	14	12	13	28	38	57	24	24	16	22	12	10	16	10	100	86	41	64	87	79	100	101	94	105	80	116	0	0.94	1
51	**R48C2-5-4**	14	13	19	32	18	12	13	28	36	77	18	18	14	18	12	12	15	25	108	79	52	68	107	106	101	98	96	90	104	100	0	0.96	1
52	R48C2-5-6	14	16	21	38	18	15	17	31	40	80	23	18	18	21	15	15	15	17	96	79	58	77	114	120	106	100	94	98	116	107	0	0.99	1
53	**R48C2-34-1***	14	15	22	40	19	15	15	30	43	84	22	23	23	27	16	14	16	15	102	89	64	97	126	113	96	92	96	107	118	114	0	0.99	1
54	**R48C2-34-4***	11	9	18	33	12	12	12	25	34	55	19	19	12	18	10	54	14	9	110	83	37	58	87	55	72	33	107	109	82	130	0	0.87	1
55	R48C2-34-12	13	14	28	42	15	15	18	31	37	56	26	26	17	24	12	70	19	13	105	77	37	56	77	40	71	26	99	108	73	119	71	0.92	1
56	R48C2-34-47	24	21	28	42	23	18	20	33	38	80	94	33	30	29	21	91	26	20	96	76	53	76	99	68	75	25	89	86	94	94	96	0.86	1
57	**R48C2-34-43***	15	15	20	32	22	15	17	29	38	77	100	26	21	19	14	72	18	12	95	70	44	77	106	67	70	24	90	91	98	101	100	0.99	1
58	R48C2-34-22	52	12	21	38	16	16	17	33	40	63	110	31	18	25	14	57	19	9	104	86	43	66	81	57	72	25	94	97	74	105	90	0.94	1
59	R48C2-34-136	43	41	53	50	34	48	46	47	51	52	103	52	38	54	33	47	50	38	90	73	42	59	63	43	61	30	86	84	60	99	45	0.83	4
60	R48C2-34-33	37	38	45	44	30	38	37	39	42	42	106	51	41	51	36	48	42	37	91	71	42	57	62	30	40	9	75	76	52	91	46	0.96	4
61	R48C1-67-48	32	32	48	57	26	41	36	33	44	43	45	32	25	37	34	50	28	21	84	75	34	52	64	18	35	3	24	11	8	96	38	0.57	3
62	R48C1-67-25	26	27	35	42	29	41	39	41	32	43	35	40	38	42	45	50	25	28	98	70	45	76	93	28	28	2	22	9	9	98	50	0.68	3
63	R48C1-67-6	35	42	39	45	38	30	32	28	30	54	36	40	46	42	41	77	21	32	90	72	46	80	94	25	34	3	20	13	12	76	44	0.92	3
64	R48C2-34-38	41	43	50	56	54	61	57	53	58	61	88	42	35	42	43	67	42	44	90	68	46	60	78	16	20	3	4	7	4	92	24	0.75	3
65	R48C2-5-49	45	41	58	67	52	67	64	57	63	59	103	32	19	27	43	50	34	29	94	62	27	47	67	22	30	3	8	8	7	93	35	0.93	3
66	R48C2-5-65	75	72	71	81	87	83	73	74	74	104	110	38	36	42	76	75	34	42	106	74	48	75	100	32	31	7	10	18	15	94	50	0.92	3
67	R48C1-67-36	36	34	39	66	65	65	67	60	65	76	46	16	15	23	50	50	29	35	107	59	33	51	99	21	22	1	9	2	2	102	47	0.88	3
68	**R48C2-5-1***	86	78	72	74	81	77	75	76	76	97	73	58	61	61	90	84	60	16	104	80	52	101	135	125	101	87	42	27	22	127	83	0.54	2
69	R48C2-34-54	80	73	69	76	75	63	71	71	72	97	95	60	64	64	73	26	26	24	97	79	64	91	114	113	95	85	26	25	27	107	93	0.95	2
70	**R48C2-5-14***	104	85	77	83	89	74	79	72	79	102	110	59	71	65	93	20	21	16	101	81	66	95	125	121	102	85	26	32	37	107	121	0.97	2
71	**R48C2-5-13***	80	67	73	71	73	65	66	67	67	81	100	54	57	62	90	18	16	13	86	69	53	80	116	117	96	77	19	25	25	100	119	0.98	2
72	R48C2-5-18	95	88	78	74	83	72	71	72	75	99	105	59	65	67	89	22	30	27	103	88	70	87	126	118	101	84	38	44	52	101	131	0.97	2
73	R48C2-5-50	77	75	63	76	72	60	63	64	73	88	115	51	57	62	78	14	12	8	108	77	69	81	112	108	99	82	21	26	28	97	117	0.97	2
74	R48C2-5-42	76	56	69	74	54	69	65	62	70	66	97	54	42	60	57	16	39	31	98	77	45	56	86	85	85	88	24	28	19	91	94	0.91	2
75	R48C2-34-32	15	12	16	55	6	5	6	9	12	49	98	54	44	58	18	5	2	2	91	65	43	48	76	69	81	66	7	11	8	93	79	0.74	-
76	R48C1-67-24	6	5	15	24	9	8	9	18	26	44	14	16	11	17	7	9	11	6	90	76	29	48	63	68	103	92	31	21	14	90	91	0.76	1
77	R48C1-67-26	6	6	10	22	9	6	7	15	21	50	10	13	13	13	15	7	9	9	103	72	41	79	125	122	99	91	36	21	21	109	131	0.94	1
78	R48C1-67-38	1	1	2	7	2	2	1	3	6	12	2	4	3	3	2	3	2	1	98	65	25	70	122	109	88	77	43	37	39	96	133	0.98	1
79	R48C2-5-28	19	11	20	33	21	14	16	28	37	53	21	26	17	25	11	16	18	12	104	81	43	51	82	81	98	93	38	27	19	101	0	0.76	1
80	R48C2-34-2	11	10	25	45	15	16	15	31	42	60	22	27	17	26	12	10	22	11	107	97	40	72	86	82	102	213	105	112	82	126	73	0.70	1
81	R48C2-34-13	12	12	22	37	16	15	17	28	37	53	21	26	17	25	11	16	18	12	104	81	43	51	82	81	98	93	38	27	19	101	0	0.76	1
82	**R48C2-5-2***	15	14	19	34	25	14	14	29	38	78	19	22	21	21	21	17	18	140	96	89	62	92	118	129	110	98	104	113	119	122	0	0.67	1
83	**R48C1-67-19***	3	4	6	49	109	175	189	199	174	63	10	4	3	4	2	6	13	128	118	109	69	7	28	20	1	4	3	3	3	2	32	-0.18	-
84	**R48C1-67-18***	160	160	199	278	243	292	303	264	265	277	213	2	1	2	90	44	56	88	101	32	3	29	41	2	3	2	2	2	1	50	4	0.66	-
	Pearson	0.98	0.97	0.95	0.92	0.97	1.00	0.98	0.99	0.78	0.57	0.53	0.81	0.95	0.74	0.35	0.36	0.72	0.06	0.38	0.61	0.82	0.84	0.82	0.84	0.88	0.59	0.98	0.91	0.50	0.39	0.04		

B

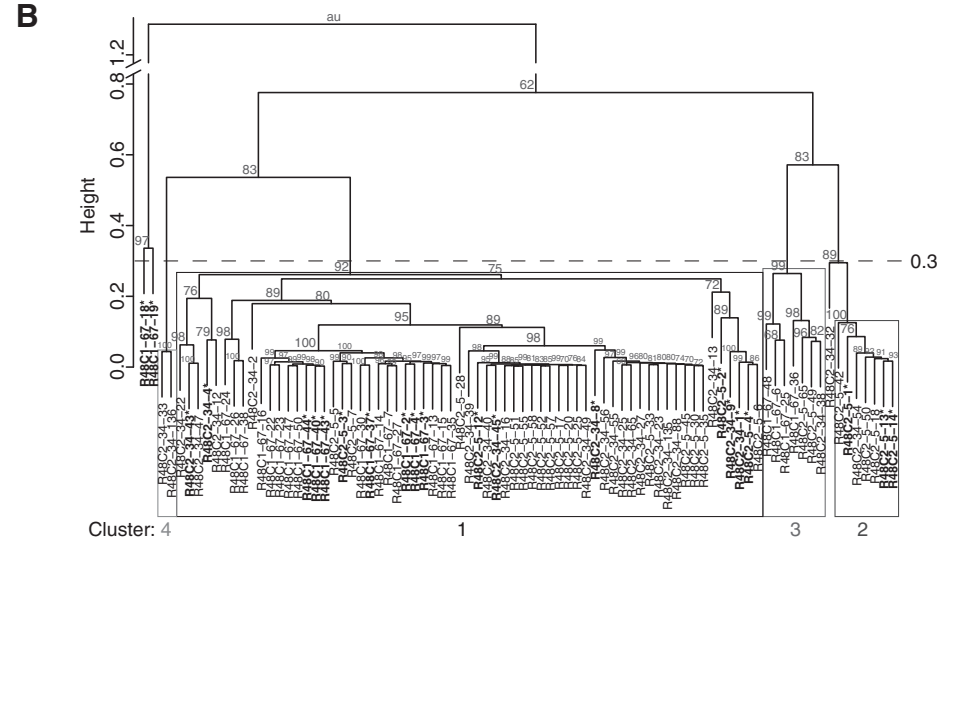

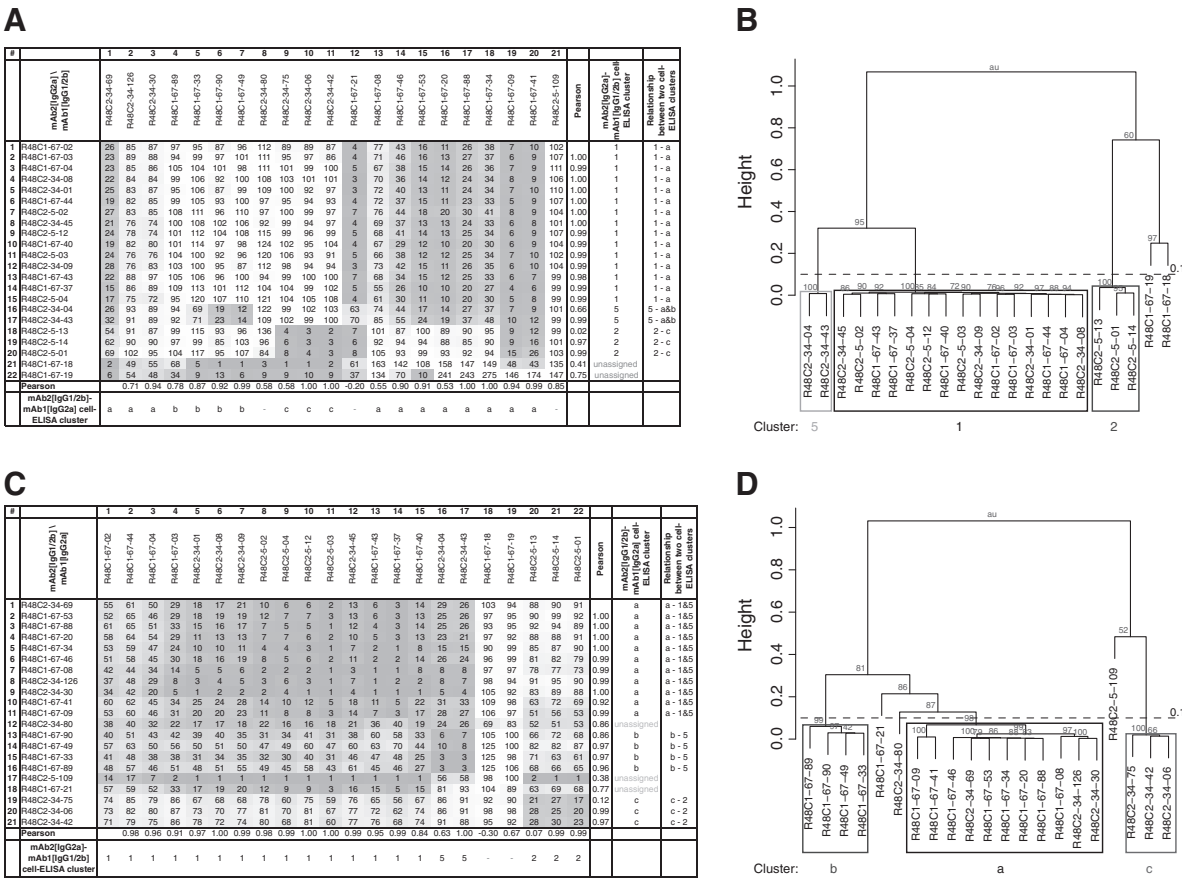

Fig. 3. Cell-based clustering assays for smaller set of mAbs in both orientations. (A, B) Twenty-two IgG2a detection mAbs profiled against twenty-one IgG1/2b blocking mAbs using the cell-based clustering assay. Two-dimensional matrix with normalized luminescence data (A) and clustergram (B) for 22 IgG2a detection mAb2's. At an AU *p*-value cut-off at 95 and a Height cut-off at 0.1, 3 clusters (1, 2 & 5) are present (B) and cluster assignment for the detection mAb2's is listed to the left of the right-most column (A). A replicate assay is shown in Supplementary Fig. 2. (C, D) Twenty-one IgG1/2b detection mAbs profiled against twenty-two IgG2a blocking mAbs using the cell-based clustering assay. Two-dimensional matrix with normalized luminescence data (C) and clustergram (D) for 21 IgG1/2b detection mAb2's. At an AU *p*-value cut-off at 95 and a Height cut-off at 0.1, 3 clusters (*a*, *b* & *c*) are present (D) and cluster assignment for the detection mAb2's is listed to the left of the right-most column (C). A replicate assay is shown in Supplementary Fig. 2. (A, C) Cluster assignments for the blocking mAb1's in the bottom-most row are based on the assays shown in D or B, respectively. The relatedness between the mAb2[IgG2a]–mAb1[IgG1/2b] clusters and the mAb2[IgG1/2b]–mAb1[IgG2a] clusters and vice versa is shown in the right-most column of both matrices. Data display and gray scaling as in Fig. 1.

shares germ-line V and J segments, has identical CDR-H3 lengths, and exhibits greater than 80% amino acid identity in CDR-H3 sequences (Poulsen et al., 2011; Wine et al., 2013). Antibodies from the same V_H clonotype likely originate from a single B-cell lineage and bind similar epitopes. Based on the analyses of antigen-mAb crystal structures an epitope that contains all contact residues is frequently 50–79 amino acids in size, whereas light and heavy chain paratopes that contain all contact residues are frequently 60–69 amino acids and 70–79 amino acids in size, respectively (Stave and Lindpaintner, 2013).

We carried out V_H sequencing to establish how cluster assignment overlaid with mAb sequence diversity. A V_H phylogram was derived to look at the relationship between all 43 DPEP1 mAbs used in the cell-based clustering assays. We categorized the mAbs according to V_H family and V_H clonotype to establish how V_H families and V_H clonotypes overlaid with the cell ELISA clusters which were established in the absence of sequence information. In Fig. 4 the 43 mAbs are ordered according to their position in the V_H phylogram. The 43 mAbs were derived from 5 different V_H gene families and 22 different V_H clonotypes: mAbs from the VHJ558 family (V_H clonotypes 1–12), the VHGAM3.8 family (V_H clonotypes 18–20) and the VH7183 family (V_H clonotype 21) fell into cell ELISA cluster 1, *a* or *c*. The VH3609 family (V_H clonotype 22) mAbs fell into cell ELISA cluster 2, whereas the VHJSM7 family (V_H clonotype 13–17) mAbs fell into cell ELISA cluster 5 or *b*. Thus, V_H usage appeared to be conserved within clusters, and mAbs that fell into the same V_H clonotype did not belong to dissimilar cell ELISA clusters. Five mAbs – R48C2-5-109, R48C1-67-21, R48C1-67-19, R48C1-67-18 and R48C2-34-80 – were not assigned to a cluster in the cell-based clustering assays. Interestingly, 3 out of these 5 mAbs – R48C2-5-109, R48C1-67-18 and R48C2-34-80 – each fell into unique V_H clonotypes. Overall, the cell-based clustering assay was able to categorize antibodies with similar sequences.

When comparing the mAb cluster assignments in all the cell ELISA assays with the mAb relatedness in the V_H phylogram,

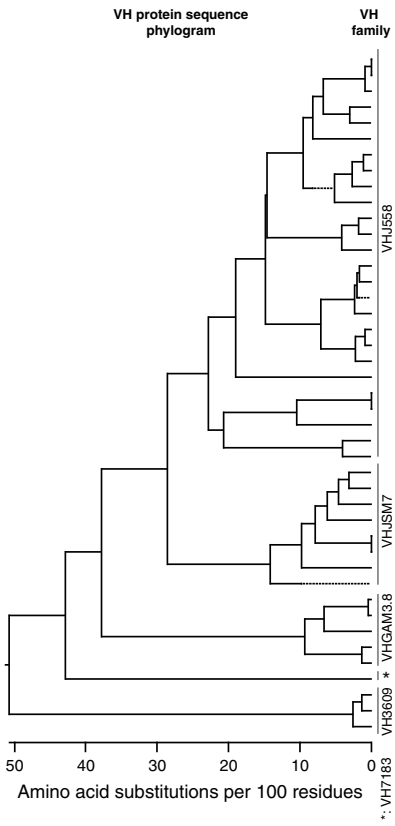

#	Hybridoma	Isotype	VH clonotypes	VH (mus IGHV[#])	JH	CDRH3 length	CDR-H3 sequence	CDRH1-H3 twin	mAb2-mAb1 cell-ELISA cluster	mAb2-mAb1 biosensor cluster	Full pairwise biosensor cluster
1	R48C2-34-6	IgG2b	1	398	JH4	12	ARGGNYYYSLDY	□	c	unassigned	unassigned
2	R48C2-34-42	IgG2b	1	398	JH4	12	ARGGNYYYSLDY	□	c	c	C
3	R48C2-34-75	IgG2b	1	398	JH4	12	ARGGNYYYSLDY		c	c	C
4	R48C1-67-8	IgG1	2	398	JH4	16	AREYFVGRYVDYAMDY		a	a	A
5	R48C1-67-46	IgG1	2	398	JH4	16	ARNYYVSRYVDYAMDY		a	a	A
6	R48C2-5-2	IgG2a	3	398	JH4	18	AREGFYRYGSIYGYGMDD		1	1	A
7	R48C2-34-1	IgG2a	4	398	JH2	14	ERSGAYITYGYFDY		1	1	A
8	R48C2-34-8	IgG2a	4	398	JH2	14	ERSGAYITYGYFDN		1	1	A
9	R48C2-34-9	IgG2a	4	398	JH2	14	GRSGAYITYGYFDY		1	1	A
10	R48C2-34-45	IgG2a	5	398	JH2	14	ARSGAYVSYGFFDY		1	1	A
11	R48C1-67-20	IgG2b	6	643	JH4	14	ARAYGYVGSYSMDY	=	a	a	A
12	R48C1-67-88	IgG2b	6	643	JH4	14	ARAYGYVGSYSMDY	=	a	a	A
13	R48C1-67-34	IgG2b	6	643	JH4	14	ARAYGYVGSYSMDY		a	a	A
14	R48C1-67-2	IgG2a	7	479	JH2	13	ARSLHYYGSKFDY	○	1	1	A
15	R48C1-67-44	IgG2a	7	479	JH2	13	ARSLHYYGSKFDY	○	1	1	A
16	R48C1-67-3	IgG2a	7	479	JH2	13	ARSLHYYGSRFDY		1	1	A
17	R48C1-67-4	IgG2a	7	479	JH2	13	ARSLHYYGSKFDY		1	1	A
18	R48C2-5-4	IgG2a	8	479	JH2	13	ARSGYYGGGYFDY	❖	1	unassigned	unassigned
19	R48C2-5-12	IgG2a	8	479	JH2	13	ARSGYYGGGYFDY	❖	1	1	A
20	R48C2-5-3	IgG2a	8	479	JH2	13	ARSGYYAGGYFDY		1	1	A
21	R48C2-5-109	IgG2b	9	286	JH2	13	ATEFITAATGLDY		unassigned	unassigned	unassigned
22	R48C1-67-43	IgG2a	10	386	JH3	15	TRGGYYYGVSRLGAY	■	1	1	A
23	R48C1-67-21	IgG2b	10	386	JH3	15	TRGGYYYGVSRLGAY	■	unassigned	a	A
24	R48C1-67-37	IgG2a	11	386	JH2	14	TRGGYFYGTKYFDF		1	1	A
25	R48C1-67-9	IgG1	12	532	JH2	11	ARGKIYDGYRY		a	a	A
26	R48C1-67-41	IgG1	12	532	JH2	11	ARGKIYDGYRY		a	a	A
27	R48C1-67-33	IgG1	13	125	JH4	11	SSLVVADAMDY		b	b	B
28	R48C1-67-89	IgG1	13	125	JH4	11	SSLVVADAMDY		b	b	B
29	R48C1-67-19	IgG2a	13	125	JH4	11	ASLVVADAMDY		unassigned	unassigned	unassigned
30	R48C1-67-90	IgG1	14	125	JH4	11	ARGGGLYALDY		b	b	B
31	R48C2-34-4	IgG2a	15	125	JH3	14	ARSRDVYYWAWFAY	◆	5	5	F
32	R48C2-34-43	IgG2a	15	125	JH3	14	ARSRDVYYWAWFAY	◆	5	5	F
33	R48C1-67-49	IgG1	16	125	JH1	13	ASNYGSFYGYFDV		b	b	B
34	R48C1-67-18	IgG2a	17	125	JH4	10	ARTGTGAMDY		unassigned	unassigned	unassigned
35	R48C2-34-30	IgG1	18	156	JH3	15	ASGANHYNYPAWFAY		a	e	E
36	R48C2-34-126	IgG1	18	156	JH3	15	ASGANHYNYPAWFAY		a	e	E
37	R48C2-34-80	IgG1	19	156	JH3	13	ARELANWDSWFTY		unassigned	unassigned	unassigned
38	R48C1-67-40	IgG2a	20	156	JH2	14	ARSGDVWFRGYFDY	⊙	1	1	A
39	R48C1-67-53	IgG1	20	156	JH2	14	ARSGDVWFRGYFDY	⊙	a	a	A
40	R48C2-34-69	IgG1	21	139	JH2	11	ARSQLRGYFDY		a	a	A
41	R48C2-5-1	IgG2a	22	433	JH4	13	VRIENIVYYAMDY		2	unassigned	unassigned
42	R48C2-5-14	IgG2a	22	433	JH4	13	VRIENMVYYAMDY		2	2	D
43	R48C2-5-13	IgG2a	22	675	JH4	13	ARIENMVYYAMDY		2	2	D

Fig. 4. V_H phylogram of 43 mAbs with V_H family, V_H clonotype, and cluster assignments. The V_H phylogram for the 43 DPEP1 mAbs was established in ClustalW by using the V_H sequencing data. To the right of the V_H phylogram 5 V_H families and 43 hybridoma names are listed. Next to the hybridoma name, isotype (IgG2a in black, IgG2a in blue, and IgG1 in green) and V_H clonotype number is presented. A V_H clonotype is a group of mAbs with the same V_H and J_H genes (listed in alternating colors — black and gray), identical CDR-H3 lengths, and at least 80% sequence identity in CDR-H3 (1-letter amino acid color coding from VBASE2 (Retter et al., 2005)). Next to the CDR-H3 sequence, we used different symbols to highlight what mAbs had the same CDR-H1, CDR-H2 and CDR-H3 sequences (i.e. CDRH1-H3 twin). MAbs with the same symbol (□, =, ○, ❖, ■, ◆, ⊙) are CDRH1-3 twins. On the right side of the table, cluster assignments from the various assays presented in Figs. 3, 5 & 6 and Supplementary Fig. 4 are shown (gray scaling of clusters as shown in respective figures).

it became apparent that V_H sequencing also enabled establishment of relationships between mAb2[IgG2a]–mAb1[IgG1/2b] and mAb2[IgG1/2b]–mAb1[IgG2a] clusters: clusters 1 & *a* were closely related and all mAbs from these clusters were derived from the VHJ558, VHGAM3.8, and VH7183 families (Fig. 4). The VHJ558 family also gave rise to cluster *c* mAbs. Cluster 5 and *b* were related and contained mAbs from the VHJSM7 family. Cluster 2 contained mAbs from the VH3609 family.

3.4. Comparison of cell-based clustering assay with a biosensor-based clustering assay

To validate the cell-based clustering assay with an established purified protein-based epitope binning assay (Abdiche et al., 2012; Abdiche et al., 2009; Estep et al., 2013), we analyzed all 43 mAbs by bio-layer interferometry (BLI) using an in-tandem assay format (Abdiche et al., 2009). After incubating the DPEP1-coated biosensor tips with the first crude hybridoma supernatant (mAb1) or media, the biosensor was dipped in the second crude hybridoma supernatant (mAb2). Sensorgram examples of 4 mAb2's profiled against 4 mAb1's are shown in Supplementary Fig. 3. All 43 mAbs were evaluated as mAb1 and mAb2 so that a full pairwise two-dimensional matrix could be constructed. The binding response profile for a mAb2 in combination with a mAb1 was normalized against the binding response profile for that same mAb2 in combination with media to control for a decrease in binding capacity of the DPEP1-coated sensors by media components.

To compare the BLI biosensor-based assay data with the cell-based assay data, the normalized responses for the IgG2a mAb2's were first graphed against the IgG1/2b mAb1's (Fig. 5A & B), followed by the normalized responses for the IgG1/2b mAb2's against the IgG2a mAb1's (Fig. 6A & B). In Fig. 5B, with an AU *p*-value cut-off at 95 and a Height cut-off at 0.2, three mAb2[IgG2a]–mAb1[IgG1/2b] biosensor clusters emerged. While eighteen IgG2a's fell into the same clusters in the cell-based and the biosensor-based assay, two mAb2's – R48C2-5-01 and R48C2-5-04 – could not be assigned to a cluster when using the biosensor-based method. In the reciprocal biosensor-based clustergram in which the IgG1/2b mAb2 relatedness was established, four clusters emerged below a Height cut-off at 0.2 with an AU *p*-value cut-off at 95 (Fig. 6B). Two IgG1/2b mAb2's – R48C2-34-126 & R48C2-34-30 –

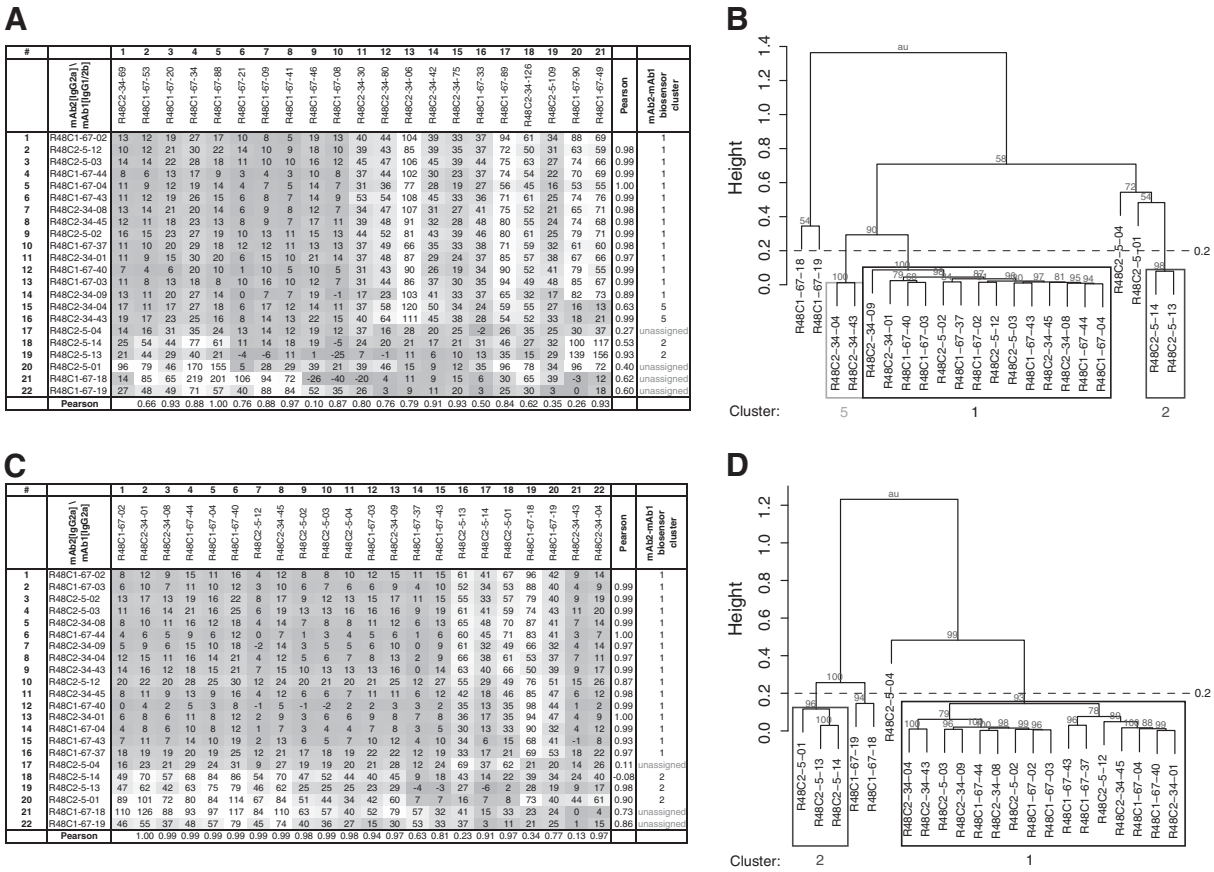

Fig. 5. Biosensor-based clustering assay for IgG2a detection mAbs. (A, B) Twenty-two IgG2a detection mAbs profiled against twenty-one IgG1/2b blocking mAbs using the biosensor-based clustering assay. Two-dimensional matrix with normalized binding response (A) and clustergram (B) for twenty-two IgG2a detection mAb2's. At an AU *p*-value cut-off at 95 and a Height cut-off at 0.2, 3 clusters (1, 2 & 5) are present in the clustergram (B) and cluster assignment for the detection mAb2's is listed in the right-most column of the matrix (A). (C, D) Twenty-two IgG2a detection mAbs profiled against same twenty-two IgG2a blocking mAbs using the biosensor-based clustering assay. Two-dimensional matrix with normalized binding response (C) and clustergram (D) for twenty-two IgG2a detection mAb2's. Two clusters are present in the clustergram (D) with a Height cut-off at 0.2: cluster 1 is defined at an AU *p*-value cut-off at 92 and cluster 2 is defined at an AU *p*-value cut-off at 95. Cluster assignment for the detection mAb2's is listed in the right-most column of the matrix (C). Data display and gray scaling as in Fig. 1.

fell into a new cluster (cluster *e*), one related to cluster *a*. While R48C1-34-6 no longer fell into cluster *c*, R48C1-67-21 was assigned to cluster *a* (Fig. 5B). The other seventeen IgG1/2b mAb2's clustered in a similar manner in the cell-based and biosensor-based assay. In light of the V_H sequencing data, it seemed more appropriate to set the Height cut-offs at 0.2 in the biosensor-based assays, because cluster fragmentation occurred at lower Height cut-offs. For example, cluster *a* in Fig. 6A fragmented into multiple clusters at a Height cut-off of 0.1 with classification of mAbs from the same V_H clonotype – R48C1-67-08 and R48C1-67-46 – into different clusters (Section 3.3). Overall, good agreement was observed between the cell-based and biosensor-based assays with Height cut-offs at 0.1 and 0.2, respectively.

A full pairwise comparison cannot be conducted when using the cell-based clustering assay, because mAbs with the same isotype cannot be tested against each other. We postulate that as long as the diversity of the blocking mAb1 collection is equivalent to the diversity of the detection mAb2 collection, a full pairwise comparison is not required. To establish whether mAb binding-site diversity was equivalent in the set of 22 IgG2a mAbs and the set of 21 IgG1/2b mAbs, we derived a two-dimensional matrix and clustergram in which the IgG2a's were profiled both as mAb1 and mAb2 (Fig. 5C & D). Clusters were defined at an AU *p*-value cut-off at 95 and a Height cut-off at 0.2, with the exception of cluster 1. In light of the V_H sequencing data, it seemed more appropriate to set the AU *p*-value cut-off for cluster 1 at 92, so that V_H clonotypes 4 & 7 did not segregate into 2 separate clusters (Section 3.3). When cluster assignments between the mAb2[IgG2a]–mAb1 [IgG1/2b] clustergram (Fig. 5B) and the mAb2[IgG2a]–mAb1 [IgG2a] clustergram (Fig. 5D) were compared, few differences were observed — cluster 5 was part of cluster 1 and R48C2-5-4 fell into cluster 2 (Fig. 5D). The two-dimensional matrix and clustergram in which the IgG1/2b mAbs were assayed both as mAb1 and mAb2 (Fig. 6C & D) were also equivalent to the matrix and clustergram in which the IgG1/2b mAbs were profiled as mAb2 against the IgG2a mAbs as mAb1 (Fig. 6A & B), with one exception — R48C1-67-21 did not fall into a cluster (Fig. 6D), similar to what was seen in the

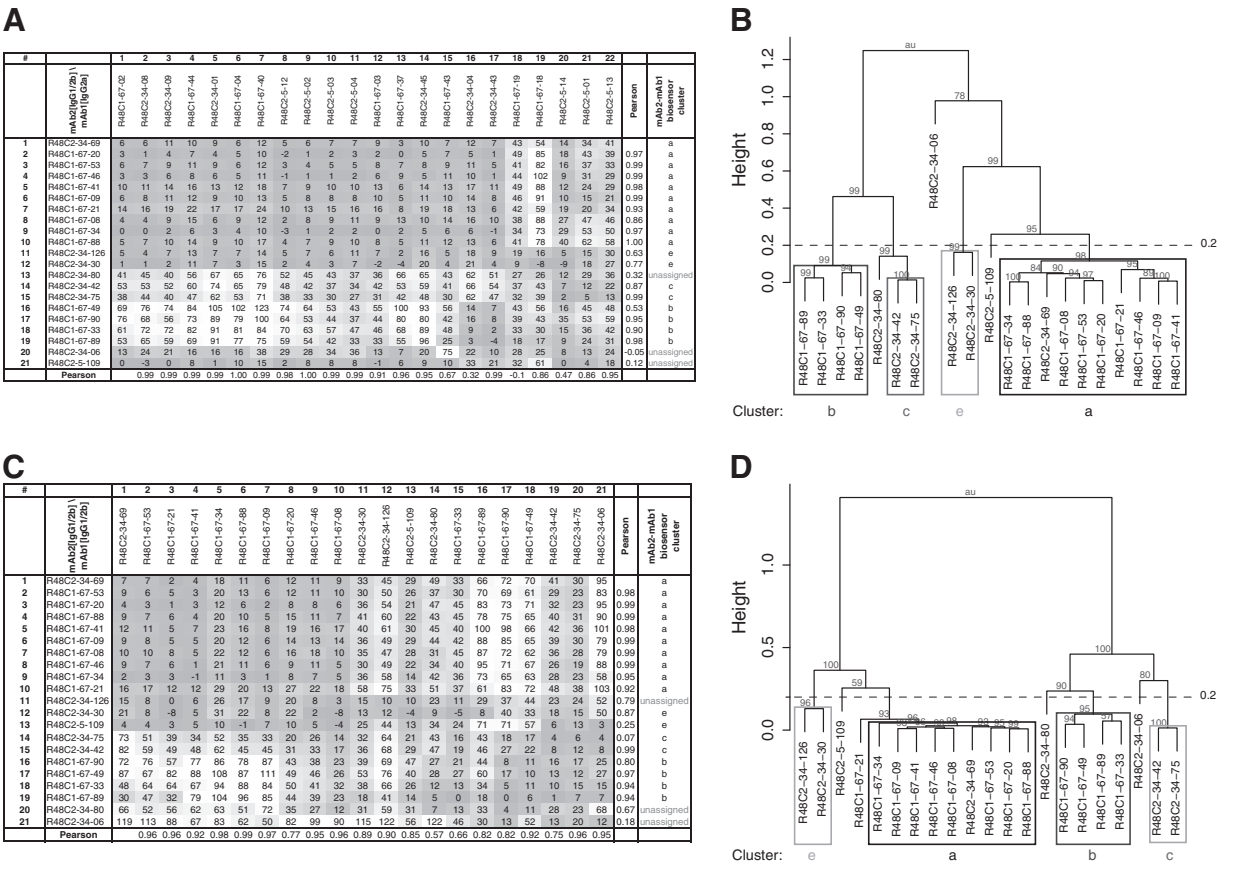

Fig. 6. Biosensor-based clustering assay for IgG1/2b detection mAbs. (A, B) Twenty-one IgG1/2b detection mAbs profiled against twenty-two IgG2a blocking mAbs using the biosensor-based clustering assay. Two-dimensional matrix with normalized binding response (A) and clustergram (B) for twenty-one IgG1/2b detection mAb2's. At an AU *p*-value cut-off at 95 and a Height cut-off at 0.2, 4 clusters (*a*, *b*, *c* & *e*) are present in the clustergram (B) and cluster assignment for the detection mAb2's is listed in the right-most column of the matrix (A). (C, D) Twenty-one IgG1/2b detection mAbs profiled against same twenty-one IgG1/2b blocking mAbs using the biosensor-based clustering assay. Two-dimensional matrix with normalized binding response (C) and clustergram (D) for 21 IgG1/2b detection mAb2's. At an AU *p*-value cut-off at 95 and a Height cut-off at 0.2, four clusters (*a*, *b*, *c* & *e*) are present in the clustergram (D) and cluster assignment for the detection mAb2's is listed in the right-most column of the matrix (C). Data display and gray scaling as in Fig. 1.

cell-based clustering assay (Fig. 3D). In conclusion, the blocking characteristics of the IgG1/2b and IgG2a collections appeared to be analogous.

Unlike cell-based clustering, biosensor-based clustering can generate a full pairwise two-dimensional matrix. All mAbs self-blocked at a cut-off of 30% normalized binding in the two-dimensional matrix (Supplementary Fig. 4A). In the mAb2 [IgG1/2a/2b]–mAb1[IgG1/2a/2b] biosensor clustergram six clusters (A, B, C, D, E & F) emerged when applying an AU *p*-value cut-off at 95 and a Height cut-off at 0.2 (Supplementary Fig. 4B). mAbs in cluster A belonged to cell ELISA clusters 1, 5 & *a* (Fig. 4). Cluster B mAbs were akin to cell ELISA cluster *b*, cluster C mAbs were equivalent to cell ELISA cluster *c*, cluster D mAbs were equivalent to cell ELISA cluster 2, cluster E was comparable to biosensor cluster *e*, and cluster F was comparable to cell ELISA cluster 5 (Fig. 4).

4. Discussion

Antibody epitope binning assays are used to characterize antibody diversity. The number of clusters identified in the epitope binning assay depends on the size of the extracellular domain(s) and the degree of amino acid identity between the human protein and the protein of the species used for immunization. In the event the mAb collection is comprised of few clusters, alternative species could be considered for immunization to derive additional mAbs.

Certain assays, like immunogenicity or receptor occupancy assays, can be developed with mAbs that bind distinct epitopes. In addition, antibody diversity can be overlaid with other data to understand whether mAbs within a subset of or all epitope clusters show the properties of interest, such as in vitro cell killing or cross-reactivity with the target in cynomolgus monkey. If mAbs from a particular cluster have desirable properties (e.g. in vitro cell killing activity), but contain amino acid sequence liabilities (e.g. glycosylation sites) in the three complementarity-determining regions, epitope binning can be conducted on new mAb collections to identify mAbs that belong to the same cluster, have the same desirable properties, but lack sequence liabilities.

Most clustering assays require purified recombinant antigen and/or purified mAbs labeled with a detection signal (Abdiche et al., 2009; Ando et al., 2004; Jia et al., 2004; Miller et al., 2011). We describe a cell ELISA-based clustering assay that

uses crude hybridoma supernatants and cells expressing the human antigen of interest. This cell-based assay can be used to screen large hybridoma collections. We show that this assay is comparable to a biosensor-based clustering assay and that the cell ELISA clusters largely parallel the mAb diversity established by V_H sequencing.

4.1. Defining mAb clusters

In this report we used a two-dimensional matrix and hierarchical clustering of the mAb1 blocking profiles to assess mAb2 diversity (Miller et al., 2011; Suzuki and Shimodaira, 2006). Clusters were defined top-down below a manually set Height cut-off on the *y*-axis with calculated AU *p*-values greater than 90 to 95. Failure to use a Height cut-off results in reporting fewer clusters that contain dissimilar mAbs. For example, without a Height cut-off, only 2 clusters with an AU *p*-value cut-off at 95 emerged in Fig. 6B: from left to right, the first cluster contained 7 mAbs, placing R48C2-34-80 and clusters *b* & *c* mAbs together. However, the blocking profiles for R48C2-34-80 and clusters *b* & *c* mAbs in the two-dimensional matrix were clearly distinct (Fig. 6A). While a Height cut-off that is too high results in establishment of clusters with dissimilar mAbs, a Height cut-off that is too low triggers the opposite — i.e. similar mAbs segregate into multiple clusters.

Furthermore, assay reproducibility and V_H sequencing on a smaller hybridoma subset can be used to set and potentially adjust the Height and AU *p*-value cut-offs. For example, the IgG2a mAb2 clusters were identical in the replicate assays at Height and AU *p*-value cut-offs at 0.1 and 95, respectively (Fig. 3B & Supplementary Fig. 2B), and appeared to be biologically meaningful, because mAbs from the same V_H clonotype did not segregate into multiple clusters (Fig. 4). Importantly, the adjusted cut-offs can be applied to the first clustering assay to re-assess mAb diversity in the large hybridoma collection. For example, the replicate assays reassign R48C2-34-4 & R48C2-34-42 to cluster 5, a cluster related to, but distinct from cluster 1 (Fig. 3B & Supplementary Fig. 2B). When inspecting cluster 1 in the large-scale clustering assay (Fig. 2B), R48C2-34-4, R48C2-34-42 and three other hybridomas (all on the far-left in cluster 1; R48C2-34-22, R48C2-34-47 and R48C2-34-12) appear to be distinct from the other hybridomas in cluster 1.

4.2. Antibodies as blocking or detection mAbs in the cell-based clustering assay

When working with mouse mAbs, an inherent feature of the cell-based clustering assay is that mAb diversity can only be interrogated between isotype classes. In the event class switch recombination is biased heavily towards a particular isotype, the method could be limiting. Alternatively, newly isolated mAbs from other species (e.g. rat or human) could easily be compared with known mouse mAbs by using the appropriate secondary antibodies.

In this report, we carry out the cell-based clustering assay in two formats by using the murine blocking mAb1's as murine detection mAb2's, and vice versa. Once all mAbs have been profiled as detection mAb2's, they are assigned to a mAb2–mAb1 cluster. We consider mAb2[IgG2a]–mAb1[IgG1/2b] clusters related to mAb2[IgG1/2b]–mAb1[IgG2a] clusters and vice versa when at least half of the blocking mAb1's from a particular cluster (blocking mAb1's assigned to clusters when assayed as detection mAb2's) block the detection mAb2's of a particular cluster by at least 50%. In the rightmost columns in Fig. 3A & C, cluster relationships were not symmetrical. For example, cluster 1 in Fig. 3A was related to cluster *a*, whereas cluster *a* in Fig. 3C was related to clusters 1 & 5. Cluster asymmetry is due to the fact that certain mAbs do not exhibit the same binding profile in both assay orientations, a phenomenon described by others as asymmetry in the blocking matrix (Abdiche et al., 2009; Nagata et al., 2004). A possible explanation for this asymmetry is that these mAbs have poor binding properties. However, the off-rates for all mAbs were reasonable (Supplementary Table 2). As an alternate explanation, epitope–paratope interaction 1 could block accessibility of epitope 2 for paratope 2 due to steric, electrostatic or allosteric effects, but the reciprocal is not necessarily true, resulting in asymmetry in the blocking matrix. To establish and validate the cell-based clustering assay we only established mAb2 clustergrams by using the mAb1 blocking profiles for the different mAb2's. However, one can also look at mAb1 relatedness by generating a clustergram using the mAb2 competition profiles for the various mAb1's.

We recommend selecting mAbs from both isotype classes for further characterization, not only to confirm mAb binding-site diversity, but also to obtain greater mAb sequence diversity. While the blocking properties of the DPEP1 IgG2a mAb and IgG1/2b mAb groups were equivalent, less sequence redundancy was observed between the two isotype classes, because somatic hypermutation occurs upon class switch recombination (Keim et al., 2013). In Fig. 4, we reported 7 pairs of CDRH1-3 twin sequences — only 2 out of the 7 pairs contain different isotypes.

4.3. V_H sequencing to corroborate cluster assignments

V_H sequencing was useful as a technique to validate mAb diversity captured by the cell-based clustering assay. Upon heavy chain variable region sequencing, we assigned antibodies to V_H families and V_H clonotypes. Because mAbs that fell into the same V_H clonotype did not belong to dissimilar cell ELISA clusters, we feel that AU *p*-value cut-offs between 90 and 95 were appropriate for mAb categorization. We reported 5 V_H families and 22 V_H clonotypes for the 43 DPEP1 antibodies used to evaluate the reproducibility of the cell-based clustering assay. V_H family usage within clusters suggested that for a given epitope, only a few members of the germ-line repertoire were used to establish the corresponding paratope. The DPEP1 hybridomas were derived from three different fusions: R48C1-67, R48C2-34 and R48C2-5. Within a specific V_H clonotype containing multiple mAbs (13 out of 22 clonotypes contain more than 1 mAb), we did not observe mAbs derived from different fusions, supporting the notion that mAbs belonging to the same V_H clonotype are derived from a single B cell lineage. Also, 3 V_H clonotypes (10, 13, 20) contained mAbs with different isotypes, further supporting the assumption that the IgG1/2b and IgG2a mAb collections contain mAbs with comparable epitopes. Two DPEP1 mAb clusters that did not undergo V_H sequencing – clusters 3 & 4 (Fig. 2B) – potentially contain additional V_H sequence diversity.

In addition, V_H sequencing was used to make adjustments to a small subset of the biosensor-based cluster assignments.

For example, we adjusted the AU *p*-value cut-off to 92 for cluster 1 in one of the biosensor-based assays (Fig. 5D), because mAbs from the same V_H clonotypes segregated at an AU *p*-value cut-off of 95.

4.4. Cell-based versus biosensor-based clustering assays

The cell-based clustering assay was validated against a biosensor-based method. Overall, mAb2 cluster assignments were similar in both assays (Fig. 4). Small differences in cluster assignments between the two assay formats could be attributable to assay-specific characteristics. While 2 mAbs – R48C2-34-30 & R48C2-34-126 – fell into cluster *a* in the cell-based assay, they fell into cluster *e* in the biosensor-based assay. Three mAbs – R48C2-34-6, R48C2-5-4, and R48C2-5-1 – fell into clusters in the cell-based assay, but could not be assigned to a cluster in the biosensor-based assay. One mAb – R48C1-67-21 – remained unassigned in the cell-based assay, and fell into cluster *a* in the biosensor-based assay. Some assay characteristics that may amplify differences between the two approaches include, but are not limited to the following: (1) turnover of the protein at the cell surface in the cell-based assay when the wash, fixation step, and wash between mAb1 and mAb2 incubation are omitted (Supplementary Fig. 1C & D); (2) non-native conformation and/or aggregated protein in the biosensor-based assay; (3) media interference in the cell-based and/or biosensor-based assay.

5. Conclusion

In this report we describe a cell-based clustering assay that enables assessment of mAb diversity in large crude hybridoma supernatant collections using engineered cells that express a human target of interest. We show that the assay is reproducible and produces results equivalent to a biosensor-based clustering assay and consistent with clustering based on V_H sequencing. Importantly, we have also successfully used the cell-based clustering assay to cluster mAb collections against various membrane proteins with multiple extracellular domains for which recombinant protein fragments are not available (data not shown). While we carried out the cell-based clustering assay with an engineered cell line, the cell-based clustering assay may be performed with established, endogenous expressing cell lines that are amenable to cell-based ELISAs.

Supplementary data to this article can be found online at http://dx.doi.org/10.1016/j.jim.2013.12.007.

Acknowledgments

We would like to thank Thi-Sau Migone, Diane Hollenbaugh and Scott Klakamp for proofreading the article, Karl Schweighofer for help with the R package pvclust for hierarchical clustering, Zhi-Wei Li for the sarcoma cell line expressing DPEP1, and Barbara Daine-Matsuoka for help with hybridoma cloning.

References

Abdiche, Y.N., Malashock, D.S., Pinkerton, A., Pons, J., 2009. Exploring blocking assays using Octet, ProteOn, and Biacore biosensors. Anal. Biochem. 386, 172.

Abdiche, Y.N., Lindquist, K.C., Stone, D.M., Rajpal, A., Pons, J., 2012. Label-free epitope binning assays of monoclonal antibodies enable the identification of antigen heterogeneity. J. Immunol. Methods 382, 101.

Ando, T., Latif, R., Daniel, S., Eguchi, K., Davies, T.F., 2004. Dissecting linear and conformational epitopes on the native thyrotropin receptor. Endocrinology 145, 5185.

Beck, A., Wurch, T., Bailly, C., Corvaia, N., 2010. Strategies and challenges for the next generation of therapeutic antibodies. Nat. Rev. Microbiol. 10, 345.

Byrd, J.C., Kipps, T.J., Flinn, I.W., Cooper, M., Odenike, O., Bendiske, J., Rediske, J., Bilic, S., Dey, J., Baeck, J., O'Brien, S., 2012. Phase I study of the anti-CD40 humanized monoclonal antibody lucatumumab (HCD122) in relapsed chronic lymphocytic leukemia. Leuk. Lymphoma 53, 2136.

Dong, J., Demarest, S.J., Sereno, A., Tamraz, S., Langley, E., Doern, A., Snipas, T., Perron, K., Joseph, I., Glaser, S.M., Ho, S.N., Reff, M.E., Hariharan, K., 2010. Combination of two insulin-like growth factor-I receptor inhibitory antibodies targeting distinct epitopes leads to an enhanced antitumor response. Mol. Cancer Ther. 9, 2593.

Estep, P., Reid, F., Nauman, C., Liu, Y., Sun, T., Sun, J., Xu, Y., 2013. High throughput solution-based measurement of antibody–antigen affinity and epitope binning. mAbs 5, 270.

Fagerstam, L.G., Frostell, A., Karlsson, R., Kullman, M., Larsson, A., Malmqvist, M., Butt, H., 1990. Detection of antigen–antibody interactions by surface plasmon resonance. Application to epitope mapping. J. Mol. Recognit. 3, 208.

Fendly, B.M., Winget, M., Hudziak, R.M., Lipari, M.T., Napier, M.A., Ullrich, A., 1990. Characterization of murine monoclonal antibodies reactive to either the human epidermal growth factor receptor or HER2/neu gene product. Cancer Res. 50, 1550.

Hellstrom, K.E., Yelton, D.E., Fell, H.P., Beaton, D., Gayle, M., MacLean, M., Kahn, M., Hellstrom, I., 1990. Epitope mapping and use of anti-idiotypic antibodies to the L6 monoclonal anticarcinoma antibody. Cancer Res. 50, 2449.

Jia, X.C., Raya, R., Zhang, L., Foord, O., Walker, W.L., Gallo, M.L., Haak-Frendscho, M., Green, L.L., Davis, C.G., 2004. A novel method of multiplexed competitive antibody binning for the characterization of monoclonal antibodies. J. Immunol. Methods 288, 91.

Jones, S.T., Bendig, M.M., 1991. Rapid PCR-cloning of full-length mouse immunoglobulin variable regions. Biotechnology 9, 579.

Keim, C., Kazadi, D., Rothschild, G., Basu, U., 2013. Regulation of AID, the B-cell genome mutator. Gene Dev. 27, 1.

Keynan, S., Asipu, A., Hooper, N.M., Turner, A.J., Blair, G.E., 1997. Stable and temperature-sensitive transformation of baby rat kidney cells by SV40 suppresses expression of membrane dipeptidase. Oncogene 15, 1241.

Koefoed, K., Steinaa, L., Soderberg, J.N., Kjaer, I., Jacobsen, H.J., Meijer, P.J., Haurum, J.S., Jensen, A., Kragh, M., Andersen, P.S., Pedersen, M.W., 2011. Rational identification of an optimal antibody mixture for targeting the epidermal growth factor receptor. mAbs 3, 584.

Matsushita, H., Vesely, M.D., Koboldt, D.C., Rickert, C.G., Uppaluri, R., Magrini, V.J., Arthur, C.D., White, J.M., Chen, Y.S., Shea, L.K., Hundal, J., Wendl, M.C., Demeter, R., Wylie, T., Allison, J.P., Smyth, M.J., Old, L.J., Mardis, E.R., Schreiber, R.D., 2012. Cancer exome analysis reveals a T-cell-dependent mechanism of cancer immunoediting. Nature 482, 400.

Miller, P.L., Wolfert, R.L., Diedrich, G., 2011. Epitope binning of murine monoclonal antibodies by a multiplexed pairing assay. J. Immunol. Methods 365, 118.

Murphy, K.P., Janeway, C., Travers, P., Walport, M., 2008. Janeway's Immunobiology, 7th edn. Garland Science, New York.

Nagata, S., Numata, Y., Onda, M., Ise, T., Hahn, Y., Lee, B., Pastan, I., 2004. Rapid grouping of monoclonal antibodies based on their topographical epitopes by a label-free competitive immunoassay. J. Immunol. Methods 292, 141.

Nakamura, G.R., Fonseca, D.P., O'Rourke, S.M., Vollrath, A.L., Berman, P.W., 2012. Monoclonal antibodies to the V2 domain of MN-rgp120: fine mapping of epitopes and inhibition of alpha4beta7 binding. PLoS ONE 7, e39045.

Niederfellner, G., Lammens, A., Mundigl, O., Georges, G.J., Schaefer, W., Schwaiger, M., Franke, A., Wiechmann, K., Jenewein, S., Slootstra, J.W., Timmerman, P., Brannstrom, A., Lindstrom, F., Mossner, E., Umana, P., Hopfner, K.P., Klein, C., 2011. Epitope characterization and crystal structure of GA101 provide insights into the molecular basis for type I/II distinction of CD20 antibodies. Blood 118, 358.

Pedersen, M.W., Jacobsen, H.J., Koefoed, K., Hey, A., Pyke, C., Haurum, J.S., Kragh, M., 2010. Sym004: a novel synergistic anti-epidermal growth factor receptor antibody mixture with superior anticancer efficacy. Cancer Res. 70, 588.

Poulsen, T.R., Jensen, A., Haurum, J.S., Andersen, P.S., 2011. Limits for antibody affinity maturation and repertoire diversification in hypervaccinated humans. J. Immunol. 187, 4229.

Retter, I., Althaus, H.H., Munch, R., Muller, W., 2005. VBASE2, an integrative V gene database. Nucleic Acids Res. 33, D671.

Scott, A.M., Wolchok, J.D., Old, L.J., 2012. Antibody therapy of cancer. Nat. Rev. Cancer 12, 278.

Shi, E., Fury, W., Li, W., Mikulka, W., Aldrich, T., Rafique, A., Chen, G., Hoffenberg, S., Daly, T.J., Radziejewski, C., 2006. Monoclonal antibody classification based on epitope-binding using differential antigen disruption. J. Immunol. Methods 314, 9.

Stave, J.W., Lindpaintner, K., 2013. Antibody and antigen contact residues define epitope and paratope size and structure. J. Immunol. 191, 1428.

Suzuki, R., Shimodaira, H., 2006. Pvclust: an R package for assessing the uncertainty in hierarchical clustering. Bioinformatics 22, 1540.

Toiyama, Y., Inoue, Y., Yasuda, H., Saigusa, S., Yokoe, T., Okugawa, Y., Tanaka, K., Miki, C., Kusunoki, M., 2011. DPEP1, expressed in the early stages of colon carcinogenesis, affects cancer cell invasiveness. J. Gastroenterol. 46, 153.

Tsuji, I., Sato, S., Otake, K., Watanabe, T., Kamada, H., Kurokawa, T., 2012. Characterization of a variety of neutralizing anti-heparin-binding epidermal growth factor-like growth factor monoclonal antibodies by different immunization methods. mAbs 4, 732.

Wagener, C., Yang, Y.H., Crawford, F.G., Shively, J.E., 1983. Monoclonal antibodies for carcinoembryonic antigen and related antigens as a model system: a systematic approach for the determination of epitope specificities of monoclonal antibodies. J. Immunol. 130, 2308.

Wine, Y., Boutz, D.R., Lavinder, J.J., Miklos, A.E., Hughes, R.A., Hoi, K.H., Jung, S.T., Horton, A.P., Murrin, E.M., Ellington, A.D., Marcotte, E.M., Georgiou, G., 2013. Molecular deconvolution of the monoclonal antibodies that comprise the polyclonal serum response. Proc. Natl. Acad. Sci. U. S. A. 110, 2993.